

# Logic and the 2-Simplicial Transformer

James Clift\*, Dmitry Doryn\*, Daniel Murfet\*, James Wallbridge\*

February 12, 2022

## Abstract

We introduce the 2-simplicial Transformer, an extension of the Transformer which includes a form of higher-dimensional attention generalising the dot-product attention, and uses this attention to update entity representations with tensor products of value vectors. We show that this architecture is a useful inductive bias for logical reasoning in the context of deep reinforcement learning.

That some deductions are genuine, while others seem to be so but are not, is evident... So it is, too, with inanimate things; for of these, too, some are really silver and others gold, while others are not and merely seem to be such to our sense.

---

Aristotle, *Sophistical refutations*, 350 BC.

## Contents

<b>1</b>	<b>Introduction</b>	<b>2</b>
<b>2</b>	<b>2-Simplicial Transformer</b>	<b>6</b>
2.1	Transformer block . . . . .	7
2.2	2-Simplicial Transformer block . . . . .	8
<b>3</b>	<b>Environment</b>	<b>11</b>
3.1	Standard BoxWorld . . . . .	12
3.2	Bridge BoxWorld . . . . .	12
<b>4</b>	<b>Agent</b>	<b>13</b>
4.1	Basic architecture . . . . .	13
4.2	Transformer blocks . . . . .	13

---

\*Listing order is alphabetical. Correspondence to d.murfet@unimelb.edu.au.

<b>5</b>	<b>Experiments</b>	<b>15</b>
<b>6</b>	<b>Analysis</b>	<b>19</b>
6.1	Attention . . . . .	19
6.1.1	1-simplicial attention of standard entities . . . . .	20
6.1.2	2-simplicial attention . . . . .	20
6.2	The plateau . . . . .	24
<b>7</b>	<b>Discussion</b>	<b>24</b>
<b>A</b>	<b>Clifford algebra</b>	<b>25</b>
<b>B</b>	<b>Logic and reinforcement learning</b>	<b>29</b>
B.1	Strategies and proof trees . . . . .	31
<b>C</b>	<b>Time adjusted performance</b>	<b>32</b>
<b>D</b>	<b>Comparison to NTM</b>	<b>32</b>
<b>E</b>	<b>Large epsilon RMSProp</b>	<b>34</b>

# 1 Introduction

Deep learning has grown to incorporate a range of differentiable algorithms for computing with learned representations. The most successful examples of such representations, those learned by convolutional neural networks, are structured by the scale and translational symmetries of the underlying space (e.g. a two-dimensional Euclidean space for images). It has been suggested that in humans the ability to make rich inferences based on abstract reasoning is rooted in the same neural mechanisms underlying relational reasoning in space [16, 19, 6, 7] and more specifically that abstract reasoning is facilitated by the learning of *structural representations* which serve to organise other learned representations in the same way that space organises the representations that enable spatial navigation [68, 41]. This raises a natural question: are there any ideas from mathematics that might be useful in designing general inductive biases for learning such structural representations?

As a motivating example we take the recent progress on natural language tasks based on the Transformer architecture [66] which simultaneously learns to represent both entities (typically words) and relations between entities (for instance the relation between “cat” and “he” in the sentence “There was a cat and he liked to sleep”). These representations of relations take the form of query and key vectors governing the passing of messages between entities; messages update entity representations over several rounds of computation until the final representations reflect not just the meaning of words but also their context in a sentence. There is some evidence that the geometry of these final representations serve

to organise word representations in a syntax tree, which could be seen as the appropriate analogue to two-dimensional space in the context of language [33].

The Transformer may therefore be viewed as an inductive bias for learning structural representations which are *graphs*, with entities as vertices and relations as edges. While a graph is a discrete mathematical object, there is a naturally associated topological space which is obtained by gluing 1-simplices (copies of the unit interval) indexed by edges along 0-simplices (points) indexed by vertices. There is a general mathematical notion of a *simplicial set* which is a discrete structure containing a set of  $n$ -simplices for all  $n \geq 0$  together with an encoding of the incidence relations between these simplices. Associated to each simplicial set is a topological space, obtained by gluing together vertices, edges, triangles (2-simplices), tetrahedrons (3-simplices), and so on, according to the instructions contained in the simplicial set. Following the aforementioned works in neuroscience [16, 19, 6, 7, 68, 41] and their emphasis on spatial structure, it is natural to ask if a *simplicial* inductive bias for learning structural representations can facilitate abstract reasoning.

With this motivation, we begin in this paper an investigation of simplicial inductive biases for abstract reasoning in neural networks, by giving a simple method for incorporating 2-simplices (which relate three entities) into the existing Transformer architecture. We call this the *2-simplicial Transformer block*. It has been established in recent work [52, 69, 67] that relational inductive biases are useful for solving problems that draw on abstract reasoning in humans. In Section 5 we show that when embedded in a deep reinforcement learning agent our 2-simplicial Transformer block confers an advantage over the ordinary Transformer block in an environment with logical structure, and on this basis we argue that further investigation of simplicial inductive biases is warranted.

**What is the 2-simplicial Transformer block?** In each iteration of a standard Transformer block a sequence of entity representations  $e_1, \dots, e_N$  are first multiplied by weight matrices to obtain query, key and value vectors  $q_i, k_i, v_i$  for  $1 \leq i \leq N$ . Updated value vectors are then computed according to the rule

$$v'_i = \sum_{j=1}^N \frac{e^{q_i \cdot k_j}}{\sum_{s=1}^N e^{q_i \cdot k_s}} v_j. \quad (1)$$

These value vectors (possibly concatenated across multiple heads) are then passed through a feedforward network and layer normalisation [3] to compute updated representations  $e'_i$  which are the outputs of the Transformer block. In each iteration of a 2-simplicial Transformer block the updated value vector  $v'_i$  also depends on higher-order terms

$$\sum_{j,k=1}^N \frac{e^{\langle p_i, l_j^1, l_k^2 \rangle}}{\sum_{s,t=1}^N e^{\langle p_i, l_s^1, l_t^2 \rangle}} B(u_j \otimes u_k) \quad (2)$$

where  $p_i, l_i^1, l_i^2, u_i$  is a second sequence of vectors derived from the entity representation  $e_i$  via multiplication with weight matrices,  $B$  is a weight tensor and the scalars  $\langle p_i, l_j^1, l_k^2 \rangle$

are the *2-simplicial attention*, viewed as logits which predict the existence of a 2-simplex with vertices  $(i, j, k)$ . The scalar triple product  $\langle a, b, c \rangle$  can be written explicitly in terms of the pairwise dot products of  $a, b, c$  (see Definition 2.5).

If the set of possible 2-simplices  $(i, j, k)$  is unconstrained the 2-simplicial Transformer block has time complexity  $O(N^3)$  as a function of the number of entities  $N$ , and this is impractical. To reduce the time complexity we introduce a set of  $M$  *virtual entities* which are updated by the ordinary attention, and restrict our 2-simplices  $(i, j, k)$  to have  $j, k$  be virtual entities; effectively we use the ordinary Transformer to predict which entities should participate in 2-simplices. Taking  $M$  to be of the order of  $\sqrt{N}$  gives the 2-simplicial Transformer block the same complexity  $O(N^2)$  as the ordinary Transformer. For a full specification of the 2-simplicial Transformer block see Section 2.2.

The architecture of our deep reinforcement learning agent largely follows [69] and the details are given in Section 4. The key difference between our *simplicial agent* and the *relational agent* of [69] is that in place of a standard Transformer block we use a 2-simplicial Transformer block. Our use of tensor products of value vectors is inspired by the semantics of linear logic in vector spaces [25, 47, 14] in which an algorithm with multiple inputs computes on the tensor product of those inputs, but this is an old idea in natural language processing, used in models including the second-order RNN [22, 50, 27, 23], multiplicative RNN [62, 36], Neural Tensor Network [60] and the factored 3-way Restricted Boltzmann Machine [51], see Appendix D. More recently tensors have been used to model predicates in a number of neural network architectures aimed at logical reasoning [55, 18]. The main novelty in our model lies in the introduction of the 2-simplicial attention, which allows these ideas to be incorporated into the Transformer architecture.

**What is the environment?** The environment in our reinforcement learning problem is a variant of the BoxWorld environment from [69]. The original BoxWorld is played on a rectangular grid populated by keys and locked boxes, with the goal being to open the box containing the Gem (represented by a white square) as shown in the sample episode of Figure 1. Locked boxes are drawn as two consecutive pixels with the lock on the right and the contents of the box (another key) on the left. Each key can only be used once. In the episode shown there is a loose pink key (marked 1) which can be used to open one of two locked boxes, obtaining in this way either key 5 or key 2<sup>1</sup>. The correct choice is 2, since this leads via the sequence of keys 3, 4 to the Gem. All other possibilities (referred to as *distractor* boxes) lead to a board configuration in which the player is unable to obtain the Gem; for further details, including the shaping of rewards, see Section 3.1.

Our variant of the BoxWorld environment, *bridge BoxWorld*, is shown in Figure 2. In each episode two keys are now required to obtain the Gem, and there are therefore two loose keys on the board. Beginning at each loose key is a *solution path* leading to one of the keys required to open the box containing the Gem, and the eponymous bridges allow the player to cross between solution paths, thereby rendering the puzzle unsolvable. For instance, in Figure 2 opening the box marked “bridge” uses up the orange key, so it is

---

<sup>1</sup>The agent sees only the colours of tiles, not the numbers which are added here for exposition.

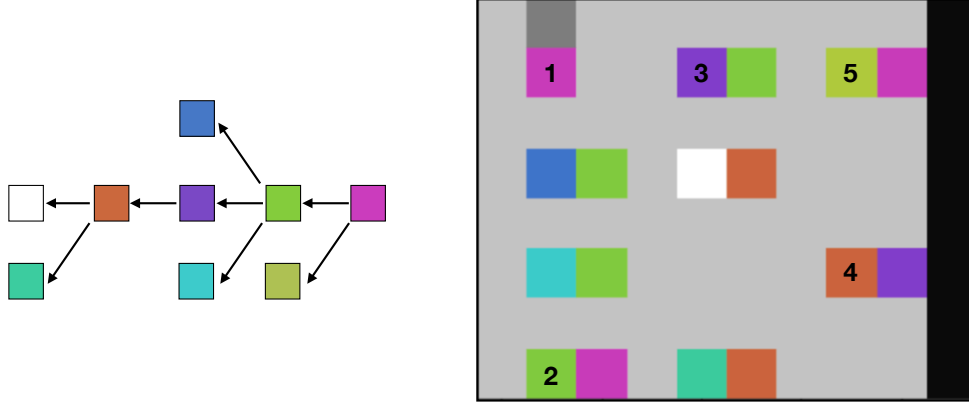


Figure 1: *Right*: a sample episode of the BoxWorld environment. Light gray tiles represent the floor, the dark gray tile is the player, the white tile is the Gem, and the rightmost column is the player inventory, currently empty. *Left*: graph representation of the puzzle, with key colours as vertices and an arrow  $C \rightarrow D$  if key  $C$  can be used to obtain key  $D$ .

only possible to obtain one of the two keys needed to open the box containing the Gem. To reach the Gem, the player must therefore learn to recognise and avoid these bridges. For further details of the bridge BoxWorld environment see Section 3.2.

**What is the logical structure of the environment?** The design of the BoxWorld environment was intended to stress the planning and reasoning components of an agent’s policy [69, p.2] and for this reason it is the underlying logical structure of the environment (rather than its representation in terms of coloured keys) that is of central importance. To explain this logical structure we introduce the following notation: given a colour  $c$ , we use  $C$  to stand for the proposition that a key of this colour is *obtainable*.

Each episode expresses its own set of basic facts, or axioms, about obtainability. For instance, a loose key of colour  $c$  gives  $C$  as an axiom, and a locked box requiring a key of colour  $c$  in order to obtain a key of colour  $d$  gives an axiom that at first glance appears to be the implication  $C \rightarrow D$  of classical logic. However, since a key may only be used once, this is actually incorrect; instead the logical structure of this situation is captured by the *linear implication*  $C \multimap D$  of linear logic [25]. With this understood, each episode of the original BoxWorld provides in visual form a set of axioms  $\Gamma$  such that a strategy for obtaining the Gem is equivalent to a proof of  $\Gamma \vdash \mathbb{G}$  in intuitionistic linear logic, where  $\mathbb{G}$  stands for the proposition that the Gem is obtainable. There is a general correspondence in logic between strategies and proofs, which we recall in Appendix B.

To describe the logical structure of bridge BoxWorld we need to encode the fact that two keys (say a green key and a blue key) are required to obtain the Gem. It is the *linear conjunction*  $\otimes$  of linear logic (also called the tensor product) rather than the conjunction of classical logic that properly captures the semantics. The axioms  $\Gamma$  encoded in an

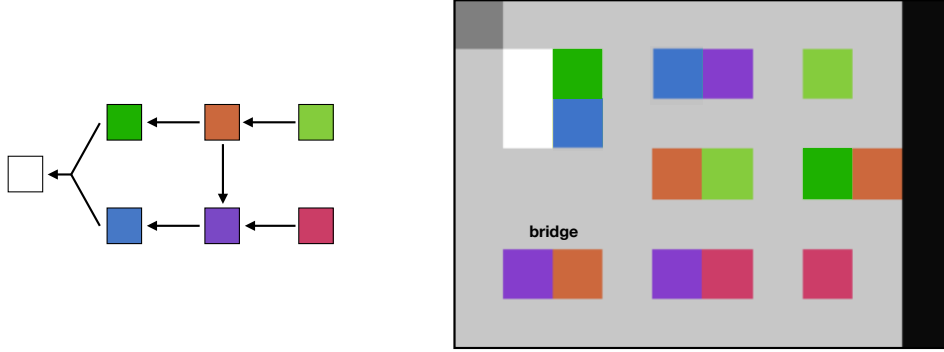


Figure 2: *Right*: a sample episode of the bridge BoxWorld environment, in which the Gem has two locks and there is a marked bridge. *Left*: graph representation of the puzzle, with upper and lower solutions paths and the bridge between them.

episode of bridge BoxWorld contain a single formula of the form  $X_1 \otimes X_2 \multimap \mathbb{G}$  where  $x_1, x_2$  are the colours of the keys on the Gem, and again a strategy is equivalent to a proof of  $\Gamma \vdash \mathbb{G}$ . In conclusion, the logical structure of the original BoxWorld consists of a fragment of linear logic containing only the connective  $\multimap$ , while bridge BoxWorld captures a slightly larger fragment containing  $\multimap$  and  $\otimes$ . The problem faced by the agent is to learn, purely through interaction, this underlying logical structure.

*Acknowledgements.* We acknowledge support from the Nectar cloud at the University of Melbourne and GCP research credits.

## 2 2-Simplicial Transformer

The Transformer architecture introduced in [66] builds on a history of attention mechanisms that in the context of natural language processing go back to [4]. For general surveys of soft attention mechanisms in deep learning see [13, 49] and [26, §12.4.5.1]. The fundamental idea, of propagating information between nodes using weights that depend on the dot product of vectors associated to those nodes, comes ultimately from statistical mechanics via the Hopfield network, see Remark 2.2. We distinguish between the *Transformer architecture* which contains a word embedding layer, an encoder and a decoder, and the *Transformer block* which is the sub-model of the encoder that is repeated.

In this section we first review the definition of the ordinary Transformer block (Section 2.1) and then explain the 2-simplicial Transformer block (Section 2.2). Both blocks define operators on sequences  $e_1, \dots, e_N$  of *entity representations*. Strictly speaking the entities are indices  $1 \leq i \leq N$  but we sometimes identify the entity  $i$  with its representation  $e_i$ . The space of entity representations is denoted  $V$ , while the space of query, key and value vectors is denoted  $H$ . We use only the vector space structure on  $V$ , but  $H = \mathbb{R}^d$  is an

inner product space with the usual dot product pairing  $(h, h') \mapsto h \cdot h'$  and in defining the 2-simplicial Transformer block we will use additional algebraic structure on  $H$ , including the “multiplication” tensor  $B : H \otimes H \rightarrow H$  of (15) (used to propagate tensor products of value vectors) and the Clifford algebra of  $H$  (used to define the 2-simplicial attention).

## 2.1 Transformer block

In the first step of the standard Transformer block we generate from each entity  $e_i$  a tuple of vectors via a learned linear transformation  $E : V \rightarrow H^{\oplus 3}$ . These vectors are referred to respectively as *query*, *key* and *value* vectors and we write

$$(q_i, k_i, v_i) = E(e_i). \quad (3)$$

Stated differently,  $q_i = W^Q e_i, k_i = W^K e_i, v_i = W^V e_i$  for weight matrices  $W^Q, W^K, W^V$ . In the second step we compute a refined value vector for each entity

$$v'_i = \sum_{j=1}^N \frac{e^{q_i \cdot k_j}}{\sum_{s=1}^N e^{q_i \cdot k_s}} v_j = \sum_{j=1}^N \text{softmax}(q_i \cdot k_1, \dots, q_i \cdot k_N)_j v_j. \quad (4)$$

Finally, the new entity representation  $e'_i$  is computed by the application of a feedforward network  $g_\theta$ , layer normalisation [3] and a skip connection

$$e'_i = \text{LayerNorm} (g_\theta(v'_i) + e_i). \quad (5)$$

We refer to this form of attention as *1-simplicial attention*.

**Remark 2.1.** At the beginning of training the query and key vectors are random vectors in  $H = \mathbb{R}^d$ , which are orthogonal in expectation if  $d$  is sufficiently large. We therefore expect that without any training  $v'_i \approx \sum_{j=1}^N \frac{1}{N} v_j$ . Suppose that for each entity  $e_i$  there is a single entity  $e_{f(i)}$  with information useful for the training objective. Then as learning progresses the random configuration  $\{(q_i, k_i)\}_{i=1}^N$  will vary so that the query  $q_i$  for entity  $e_i$  lies in the same direction as the key  $k_{f(i)}$  of  $e_{f(i)}$  and  $q_i$  is orthogonal to  $k_j$  for  $j \neq f(i)$ . Then  $\frac{e^{q_i \cdot k_{f(i)}}}{\sum_{l=1}^N e^{q_i \cdot k_l}}$  will dominate the distribution and  $v'_i \approx v_{f(i)}$ .

**Remark 2.2.** The continuous Hopfield network [34] [43, Ch.42] with  $N$  nodes updates in each timestep a sequence of vectors  $\{e_i\}_{i=1}^N$  by the rules

$$e'_i = \tanh \left[ \eta \sum_j (e_i \cdot e_j) e_j \right] \quad (6)$$

for some parameter  $\eta$ . The Transformer block may therefore be viewed as a refinement of the Hopfield network, in which the three occurrences of entity vectors in (6) are replaced by query, key and value vectors  $W^Q e_i, W^K e_j, W^V e_j$  respectively, the nonlinearity is replaced by a feedforward network with multiple layers, and the dynamics are stabilised by layer normalisation. The initial representations  $e_i$  also incorporate information about the underlying lattice, via the positional embeddings.

**Remark 2.3.** In *multiple-head* attention with  $K$  heads, there are  $K$  channels along which to propagate information between every pair of entities, each of dimension  $\dim(H)/K$ . More precisely, we choose a decomposition  $H = H_1 \oplus \cdots \oplus H_K$  so that

$$E : V \longrightarrow \bigoplus_{u=1}^K (H_u^{\oplus 3})$$

and write

$$(q_{i,(1)}, k_{i,(1)}, v_{i,(1)}, \dots, q_{i,(K)}, k_{i,(K)}, v_{i,(K)}) = E(e_i).$$

To compute the output of the attention, we take a direct sum of the value vectors propagated along every one of these  $K$  channels, as in the formula

$$e'_i = \text{LayerNorm} \left( g_\theta \left[ \bigoplus_{u=1}^K \sum_{j=1}^N \text{softmax}(q_{i,(u)} \cdot k_{1,(u)}, \dots, q_{i,(u)} \cdot k_{N,(u)})_j v_{j,(u)} \right] + e_i \right). \quad (7)$$

**Remark 2.4.** In the introduction we referred to the idea that a Transformer model learns *representations of relations*. To be more precise, these representations are *heads*, each of which determines an independent set of transformations  $W^Q, W^K, W^V$  which extract queries, keys and values from entities. Thus a head determines not only which entities are related (via  $W^Q, W^K$ ) but also what information to transmit between them (via  $W^V$ ).

The idea that the structure of a sentence acts to *transform* the meaning of its parts is due to Frege [21] and underlies the denotational semantics of logic. From this point of view the Transformer architecture is an inheritor both of the logical tradition of denotational semantics, and of the statistical mechanics tradition via Hopfield networks.

## 2.2 2-Simplicial Transformer block

In combinatorial topology the canonical one-dimensional object is the 1-simplex (or edge)  $j \longrightarrow i$  and the canonical two-dimensional object is the 2-simplex (or triangle) which we may represent diagrammatically in terms of indices  $i, j, k$  as

$$\begin{array}{ccc} & j & \\ k \swarrow & & \searrow i \\ & i & \end{array} \quad (8)$$

It is natural to apply the theory of simplicial sets and simplicial complexes, which are the mathematical objects which organise collections of  $n$ -simplices, in the context of learning representations in computer vision and machine learning, and indeed this has been done [11, 39, 8]. To the extent that our approach differs from these earlier works, the difference lies in the fact that our simplices arise from the geometric algebra of configurations of query and key vectors, which seems to be an emerging idiom within deep learning.



In the 2-simplicial Transformer block, in addition to the 1-simplicial contribution, each entity  $e_i$  is updated as a function of pairs of entities  $e_j, e_k$  using the tensor product of value vectors  $u_j \otimes u_k$  and a probability distribution derived from a scalar triple product  $\langle p_i, l_j^1, l_k^2 \rangle$  in place of the scalar product  $q_i \cdot k_j$ . This means that we associate to each entity  $e_i$  a four-tuple of vectors via a learned linear transformation  $E : V \rightarrow H^{\oplus 4}$ , denoted

$$(p_i, l_i^1, l_i^2, u_i) = E(e_i). \quad (9)$$

We still refer to  $p_i$  as the *query*,  $l_i^1, l_i^2$  as the *keys* and  $u_i$  as the *value*. Stated differently,  $p_i = W^P e_i, l_i^1 = W^{L_1} e_i, l_i^2 = W^{L_2} e_i$  and  $u_i = W^U e_i$  for weight matrices  $W^P, W^{L_1}, W^{L_2}, W^U$ .

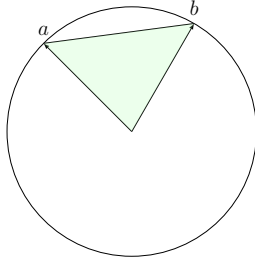
**Definition 2.5.** The *unsigned scalar triple product* of  $a, b, c \in H$  is

$$\langle a, b, c \rangle = \|(a \cdot b)c - (a \cdot c)b + (b \cdot c)a\| \quad (10)$$

whose square is a polynomial in the pairwise dot products

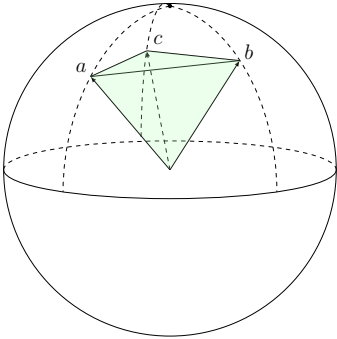
$$\langle a, b, c \rangle^2 = (a \cdot b)^2(c \cdot c) + (b \cdot c)^2(a \cdot a) + (a \cdot c)^2(b \cdot b) - 2(a \cdot b)(a \cdot c)(b \cdot c). \quad (11)$$

This scalar triple product has a simple geometric interpretation in terms of the volume of the tetrahedron with vertices  $0, a, b, c$ . To explain, recall that the triangle spanned by two unit vectors  $a, b$  in  $\mathbb{R}^2$  has an area  $A$  given by the following formula:



$$(a \cdot b)^2 = 1 - 4A^2 \quad (12)$$

In three dimensions, the analogous formula involves the volume  $V$  of the tetrahedron with vertices given by unit vectors  $a, b, c$  and the scalar triple product:



$$\langle a, b, c \rangle^2 = 1 - 36V^2 \quad (13)$$

In general, given nonzero vectors  $a, b, c$  let  $\hat{a}, \hat{b}, \hat{c}$  denote unit vectors in the same directions. We can by Lemma A.10(v) factor out the length in the scalar triple product

$$\langle a, b, c \rangle = \|a\| \|b\| \|c\| \langle \hat{a}, \hat{b}, \hat{c} \rangle \quad (14)$$

so that a general scalar triple product can be understood in terms of the vector norms and configurations of three points on the 2-sphere. One standard approach to calculating volumes of such tetrahedrons is the cross product which is only defined in three dimensions. Since the space of representations  $H$  is high dimensional the natural framework for the triple scalar product  $\langle a, b, c \rangle$  is instead the Clifford algebra of  $H$  (see Appendix A).

For present purposes, we need to know that  $\langle a, b, c \rangle$  attains its minimum value (which is zero) when  $a, b, c$  are pairwise orthogonal, and attains its maximum value (which is  $\|a\| \|b\| \|c\|$ ) if and only if  $\{a, b, c\}$  is linearly dependent (Lemma A.10). Using the number  $\langle p_i, l_j^1, l_k^2 \rangle$  as a measure of the degree to which entity  $i$  is attending to  $(j, k)$ , or put differently, the degree to which the network predicts the existence of a 2-simplex  $(i, j, k)$ , the update rule for the entities when using purely 2-simplicial attention is

$$v'_i = \sum_{j,k=1}^N \frac{e^{\langle p_i, l_j^1, l_k^2 \rangle}}{\sum_{s,t=1}^N e^{\langle p_i, l_s^1, l_t^2 \rangle}} B(u_j \otimes u_k) \quad (15)$$

where  $B : H \otimes H \rightarrow H$  is a learned linear transformation. Although we do not impose any further constraints, the motivation here is to equip  $H$  with the structure of an algebra; in this respect we model conjunction by multiplication, an idea going back to Boole [9].

We compute multiple-head 2-simplicial attention in the same way as in the 1-simplicial case. To combine 1-simplicial heads (that is, ordinary Transformer heads) and 2-simplicial heads we use separate inner product spaces  $H^1, H^2$  for each simplicial dimension, so that there are learned linear transformations  $E^1 : V \rightarrow (H^1)^{\oplus 3}, E^2 : V \rightarrow (H^2)^{\oplus 4}$  and the queries, keys and values are extracted from an entity  $e_i$  according to

$$\begin{aligned} (q_i, k_i, v_i) &= E^1(e_i), \\ (p_i, l_i^1, l_i^2, u_i) &= E^2(e_i). \end{aligned}$$

The update rule (for a single head in each simplicial dimension) is then:

$$v'_i = \left\{ \sum_{j=1}^N \frac{e^{q_i \cdot k_j}}{\sum_{s=1}^N e^{q_i \cdot k_s}} v_j \right\} \oplus \text{LayerNorm} \left\{ \sum_{j,k=1}^N \frac{e^{\langle p_i, l_j^1, l_k^2 \rangle}}{\sum_{s,t=1}^N e^{\langle p_i, l_s^1, l_t^2 \rangle}} B(u_j \otimes u_k) \right\}, \quad (16)$$

$$e'_i = \text{LayerNorm} (g_\theta(v'_i) + e_i). \quad (17)$$

Regarding the layer normalisation on the output of the 2-simplicial head see Remark 4.1. If there are  $K_1$  heads of 1-simplicial attention and  $K_2$  heads of 2-simplicial attention, then (16) is modified in the obvious way using  $H^1 = \bigoplus_{u=1}^{K_1} H_u^1$  and  $H^2 = \bigoplus_{u=1}^{K_2} H_u^2$ .

The time complexity of 1-simplicial attention as a function of the number of entities is  $O(N^2)$  while the time complexity of 2-simplicial attention is  $O(N^3)$  since we have to

calculate the attention for every triple  $(i, j, k)$  of entities. For this reason we consider only triples  $(i, j, k)$  where the base of the 2-simplex  $(j, k)$  is taken from a set of pairs predicted by the ordinary attention, which we view as the primary locus of computation. More precisely, we introduce in addition to the  $N$  entities (now referred to as *standard* entities) a set of  $M$  *virtual* entities  $e_{N+1}, \dots, e_{N+M}$ . These virtual entities serve as a “scratch pad” onto which the iterated ordinary attention can write representations, and we restrict  $j, k$  to lie in the range  $N < j, k \leq N + M$  so that only value vectors obtained from virtual entities are propagated by the 2-simplicial attention.

With virtual entities the update rule is for  $1 \leq i \leq N$

$$v'_i = \left\{ \sum_{j=1}^N \frac{e^{q_i \cdot k_j}}{\sum_{s=1}^N e^{q_i \cdot k_s}} v_j \right\} \oplus \text{LayerNorm} \left\{ \sum_{j,k=N+1}^{N+M} \frac{e^{\langle p_i, l_j^1, l_k^2 \rangle}}{\sum_{s,t=1}^{N+M} e^{\langle p_i, l_s^1, l_t^2 \rangle}} B(u_j \otimes u_k) \right\} \quad (18)$$

and for  $N < i \leq N + M$

$$v'_i = \left\{ \sum_{j=1}^{N+M} \frac{e^{q_i \cdot k_j}}{\sum_{s=1}^{N+M} e^{q_i \cdot k_s}} v_j \right\} \oplus \text{LayerNorm}(u_i). \quad (19)$$

The updated representation  $e'_i$  is computed from  $v'_i, e_i$  using (17) as before. Observe that the virtual entities are not used to update the standard entities during 1-simplicial attention and the 2-simplicial attention is not used to update the virtual entities; instead the second summand in (19) involves the vector  $u_i = W^U e_i$ , which adds recurrence to the update of the virtual entities. After the attention phase the virtual entities are discarded.

The method for updating the virtual entities is similar to the role of the memory nodes in the relational recurrent architecture of [53], the master node in [24, §5.2] and memory slots in the Neural Turing Machine [28]. The update rule has complexity  $O(NM^2)$  and so if we take  $M$  to be of order  $\sqrt{N}$  we get the desired complexity  $O(N^2)$ .

**Remark 2.6.** In the dot product attention  $q \cdot k = \|q\| \|k\| \cos(\theta)$  the norms of the queries and keys affect the distribution

$$\left\{ \frac{e^{q_i \cdot k_j}}{\sum_l e^{q_i \cdot k_l}} \right\}_{j=1}^N = \left\{ \frac{e^{\|q_i\| \|k_j\| \cos(\theta_{ij})}}{\sum_l e^{q_i \cdot k_l}} \right\}_{j=1}^N \quad (20)$$

in different ways. Since  $i$  is fixed,  $\|q_i\|$  acts like the inverse temperature in the Boltzmann distribution: increasing the query norm decreases the entropy of the distribution. On the other hand, if  $\|k_j\|$  is large then, all else being equal, any entity  $i$  which attends to  $j$  will do so strongly, and in this sense the key norm is a measure of the *importance* of entity  $j$ . Using (14) a similar interpretation applies to the 2-simplicial attention.

### 3 Environment

Our environment is an extension of the BoxWorld environment of [69], see also [53, 30], implemented as an OpenAI gym environment [10]. We begin by explaining our imple-

mentation of the original BoxWorld, and then we explain the extension used in our experiments. The code for our implementation of the original BoxWorld environment, and of bridge BoxWorld, is available online [15].

### 3.1 Standard BoxWorld

The standard BoxWorld environment is a rectangular grid in which are situated the *player* (a dark gray tile) and a number of *locked boxes* represented by a pair of horizontally adjacent tiles with a tile of colour  $x$ , the *key colour*, on the left and a tile of colour  $y$ , the *lock colour*, on the right. There is also one *loose key* in each episode, which is a coloured tile not initially adjacent to any other coloured tile. All other tiles are blank (light gray) and are traversable by the player. The rightmost column of the screen is the *inventory*, which fills from the top and contains keys that have been collected by the player. The player can pick up any loose key by walking over it. In order to open a locked box, with key and lock colours  $x, y$  as above, the player must step on the lock while in possession of a copy of  $y$ , in which case one copy of this key is removed from the inventory and replaced by a key of colour  $x$ . The goal is to attain a white key, referred to as the *Gem*.

Some locked boxes, if opened, provide keys that are not useful for attaining the Gem. Since each key may only be used once, opening such boxes means the episode is rendered unsolvable. Such boxes are called *distractors*. An episode ends when the player either obtains the Gem (with a reward of +10) or opens a distractor box (reward  $-1$ ). Opening any non-distractor box, or picking up a loose key, garners a reward of +1. The *solution length* is the number of locked boxes (including the one with the Gem) in the episode on the path from the loose key to the Gem. The episode in Figure 1 has solution length four. Episodes are parametrised by the solution length and the number of distractors.

### 3.2 Bridge BoxWorld

In our extension of the original BoxWorld environment, the box containing the Gem has two locks (of different colours). To obtain the Gem, the player must step on either of the lock tiles with both keys in the inventory, at which point the episode ends with the usual +10 reward. Graphically, Gems with multiple locks are denoted with two vertical white tiles on the left, and the two lock tiles on the right; see Figure 2.

Two solution paths (of the same length) leading to each of the locks on the Gem are generated with no overlapping colours, beginning with two loose keys. In episodes with multiple locks we do not consider distractor boxes of the old kind; instead there is a new type of distractor that we call a *bridge*. This is a locked box whose lock colour is taken from one solution branch and whose key colour is taken from the other branch. Opening the bridge renders the puzzle unsolvable. An episode ends when the player either obtains the Gem (reward +10) or opens a bridge (reward  $-1$ ). Opening a box other than the bridge, or picking up a loose key, has a reward of +1 as before. In this paper we consider episodes with zero or one bridge (the player cannot fail to solve an episode with no bridge).

## 4 Agent

Our baseline relational agent is modeled closely on [69] except that we found that a different arrangement of layer normalisations worked better in our experiments, see Remark 4.2. The code for our implementation of both agents is available online [15].

### 4.1 Basic architecture

In the following we describe the network architecture of both the relational and simplicial agent; we will note the differences between the two models as they arise. The input to the agent’s network is an RGB image, represented as a tensor of shape  $[R, C + 1, 3]$  (i.e. an element of  $\mathbb{R}^R \otimes \mathbb{R}^{C+1} \otimes \mathbb{R}^3$ ) where  $R$  is the number of rows and  $C$  the number of columns (the  $C + 1$  is due to the inventory). This tensor is divided by 255 and then passed through a  $2 \times 2$  convolutional layer with 12 features, and then a  $2 \times 2$  convolutional layer with 24 features. Both activation functions are ReLU and the padding on our convolutional layers is “valid” so that the output has shape  $[R - 2, C - 1, 24]$ . We then multiply by a weight matrix of shape  $24 \times 62$  to obtain a tensor of shape  $[R - 2, C - 1, 62]$ . Each feature vector has concatenated to it a two-dimensional positional encoding, and then the result is reshaped into a tensor of shape  $[N, 64]$  where  $N = (R - 2)(C - 1)$  is the number of Transformer entities. This is the list  $(e_1, \dots, e_N)$  of entity representations  $e_i \in V = \mathbb{R}^{64}$ .

In the case of the simplicial agent, a further two learned embedding vectors  $e_{N+1}, e_{N+2}$  are added to this list; these are the virtual entities. So with  $M = 0$  in the case of the relational agent and  $M = 2$  for the simplicial agent, the entity representations form a tensor of shape  $[N + M, 64]$ . This tensor is then passed through two iterations of the Transformer block (either purely 1-simplicial in the case of the relational agent, or including both 1 and 2-simplicial attention in the case of the simplicial agent). In the case of the simplicial agent the virtual entities are then discarded, so that in both cases we have a sequence of entities  $e''_1, \dots, e''_N$ .

To this final entity tensor we apply max-pooling over the entity dimension, that is, we compute a vector  $v \in \mathbb{R}^{64}$  by the rule  $v_i = \max_{1 \leq j \leq N} (e''_j)_i$  for  $1 \leq i \leq 64$ . This vector  $v$  is then passed through four fully-connected layers with 256 hidden nodes and ReLU activations. The output of the final fully-connected layer is multiplied by one  $256 \times 4$  weight matrix to produce logits for the actions (left, up, right and down) and another  $256 \times 1$  weight matrix to produce the value function.

### 4.2 Transformer blocks

The input to our Transformer blocks are tensors of shape  $[N, 64]$ , and the outputs have the same shape. Inside each block are two feedforward layers separated by a ReLU activation with 64 hidden nodes; the weights are shared between iterations of the Transformer block. The pseudo-code for the ordinary Transformer block inside the relational agent is:

```

def transformer_block(e):
    x = LayerNorm(e)
    a = 1SimplicialAttention(x)
    b = DenseLayer1(a)
    c = DenseLayer2(b)
    r = Add([e, c])
    eprime = LayerNorm(r)
    return eprime

```

In the 2-simplicial Transformer block the input tensor, after layer normalisation, is passed through the 2-simplicial attention and the result (after an additional layer normalisation) is concatenated to the output of the 1-simplicial attention heads before being passed through the feedforward layers:

```

def simplicial_transformer_block(e):
    x = LayerNorm(e)
    a1 = 1SimplicialAttention(x)
    a2 = 2SimplicialAttention(x)
    a2n = LayerNorm(a2)
    ac = Concatenate([a1, a2n])
    b = DenseLayer1(ac)
    c = DenseLayer2(b)
    r = Add([e, c])
    eprime = LayerNorm(r)
    return eprime

```

Our implementation of the standard Transformer block is based on an implementation in Keras from [46]. In the reported experiments we use only two Transformer blocks; we performed two trials of a relational agent using four Transformer blocks, but after  $5.5 \times 10^9$  timesteps neither trial exceeded the 0.85 plateau in terms of fraction solved. In both the relational and simplicial agent, the space  $V$  of entity representations has dimension 64 and we denote by  $H^1, H^2$  the spaces of 1-simplicial and 2-simplicial queries, keys and values. In both the relational and simplicial agent there are two heads of 1-simplicial attention,  $H^1 = H_1^1 \oplus H_2^1$  with  $\dim(H_i^1) = 32$ . In the simplicial agent there is a single head of 2-simplicial attention with  $\dim(H^2) = 48$  and two virtual entities.

**Remark 4.1.** Without the additional layer normalisation on the output of the 2-simplicial attention we find that training is unstable. The natural explanation is that these outputs are constructed from polynomials of higher degree than the 1-simplicial attention, and thus computational paths that go through the 2-simplicial attention will be more vulnerable to exploding or vanishing gradients. Ignoring denominators in the softmax and layer normalisations, the contribution to  $e'_i$  from the 1-simplicial head in (17),(18) is

$$\sum_j (1 + (q_i \cdot k_j) + \frac{1}{2}(q_i \cdot k_j)^2 + \dots) v_j \quad (21)$$

while the contribution from the 2-simplicial head is

$$\sum_{j,k} (1 + \langle p_i, l_j^1, l_k^2 \rangle + \frac{1}{2} \langle p_i, l_j^1, l_k^2 \rangle^2 + \dots) B(u_j \otimes u_k). \quad (22)$$

The lowest order term in (21) is  $v_j$  which is linear in the components of the entity vector  $e_i$ , whereas the lowest order term of (22) is  $B(u_j \otimes u_k)$  which is quadratic.

**Remark 4.2.** There is wide variation in the use of layer normalisation in the literature on Transformer models, compare [66, 12, 69]. The architecture described in [69] involves layer normalisation in two places: on the concatenation of the  $Q, K, V$  matrices, and on the output of the feedforward network  $g_\theta$ . We keep this second normalisation but move the first from *after* the linear transformation  $E$  of (3) to *before* this linear transformation, so that it is applied directly to the incoming entity representations.

We found that this works well, but the arrangement is strange in that there are two consecutive layer normalisations between iterations of the Transformer block. Note that if two layer normalisations with bias-gain pairs  $(b, g), (b', g')$  are applied in succession, then the output of the first normalisation layer on input  $x$  with mean  $b$  and variance  $\sigma^2$  will be  $x' = \frac{g}{\sigma}(x - \mu) + b$  and passing this through the second normalisation layer yields the output  $x'' = \frac{g'}{\sigma}(x - \mu) + b' - \frac{g'b}{g}$  which is equivalent to a single layer normalisation with a pair  $(b' - \frac{g'b}{g}, g')$ . It is possible the appearance of the parameter  $g$  in a nonlinear way provides a useful reparametrisation of the network [26, §8.7.1].

## 5 Experiments

The training of our agents uses the implementation in Ray RLlib [40] of the distributed off-policy actor-critic architecture IMPALA of [20] with optimisation algorithm RMSProp. The hyperparameters for IMPALA and RMSProp are given in Table 1. Following [69] and other recent work in deep reinforcement learning we use RMSProp with a large value of the hyperparameter  $\varepsilon = 0.1$ , which is *a priori* quite strange. However, as we explain in Appendix E, this is effectively a variant of RMSProp with smoothed gradient clipping.

Hyperparameter	Value
IMPALA entropy	$5 \times 10^{-3}$
Discount factor $\gamma$	0.99
Unroll length	40 timesteps
Batch size	1280 timesteps
Learning rate	$2 \times 10^{-4}$
RMSProp momentum	0
RMSProp $\varepsilon$	0.1
RMSProp decay	0.99

Table 1: Hyperparameters for agent training.



First we verified that our implementation of the relational agent can solve the standard BoxWorld environment [69] with a solution length sampled from  $[1, 5]$  and number of distractors sampled from  $[0, 4]$  on a  $9 \times 9$  grid. After training for  $2.35 \times 10^9$  timesteps our implementation solved over 93% of puzzles (regarding the discrepancy with the reported sample complexity in [69] see Remark 5.1). Next we trained the relational and simplicial agent on bridge BoxWorld, under the following conditions: half of the episodes contain a bridge, the solution length is uniformly sampled from  $[1, 3]$  (both solution paths are of the same length), colours are uniformly sampled from a set of 20 colours<sup>2</sup> and the boxes and loose keys are arranged randomly on a  $7 \times 9$  grid, under the constraint that the box containing the Gem does not occur in the rightmost column or bottom row, and keys appear only in positions  $(y, x) = (2r, 3c - 1)$  for  $1 \leq r \leq 3, 1 \leq c \leq 3$ . The starting and ending point of the bridge are uniformly sampled with no restrictions (e.g. the bridge can involve the colours of the loose keys and locks on the Gem) but the lock colour is always on the top solution path. There is no curriculum and no cap on timesteps per episode. We trained four independent trials of both agents to either  $5.5 \times 10^9$  timesteps or convergence, whichever came first. The training runs for the relational and simplicial agents are shown in Figure 4 and Figure 5 respectively. In Figure 3 we give the mean and standard deviation of these four trials of each agent, showing a clear advantage of the simplicial agent. We make some remarks about performance comparisons taking into account the fact that the relational agent is simpler (and hence faster to execute) than the simplicial agent in Appendix C.

**Remark 5.1.** The experiments in the original BoxWorld paper [69] contain an unreported cap on timesteps per episode (an *episode horizon*) of 120 timesteps [54]. We have chosen to run our experiments without an episode horizon, and since this means our reported sample complexities diverge substantially from the original paper (some part of which it seems reasonable to attribute to the lack of horizon) it is necessary to justify this choice.

When designing an architecture for deep reinforcement learning the goal is to reduce the expected generalisation error [26, §8.1.1] with respect to some class of similar environments. Although this class is typically difficult to specify and is often left implicit, in our case the class includes a range of visual logic puzzles involving spatial navigation, which can be solved without memory<sup>3</sup>. A learning curriculum undermines this goal, by making our expectations of generalisation conditional on the provision of a suitable curriculum, whose existence for a given member of the problem class may not be clear in advance. The episode horizon serves as a *de facto* curriculum, since early in training it biases the distribution of experience rollouts towards the initial problems that an agent has to solve (e.g. learning to pick up the loose key). In order to avoid compromising our ability to expect generalisation to similar puzzles which do not admit such a useful curriculum, we

---

<sup>2</sup>Saturation 0.7, brightness 0.8 and hue  $\frac{18k}{360}$  for  $0 \leq k \leq 19$ .

<sup>3</sup>The bridge is the unique box both of whose colours appear three times on the board. However, this is not a reliable strategy for detecting bridges for an agent without memory, because once the agent has collected some of the keys on the board, some of the colours necessary to make this deduction may no longer be present.



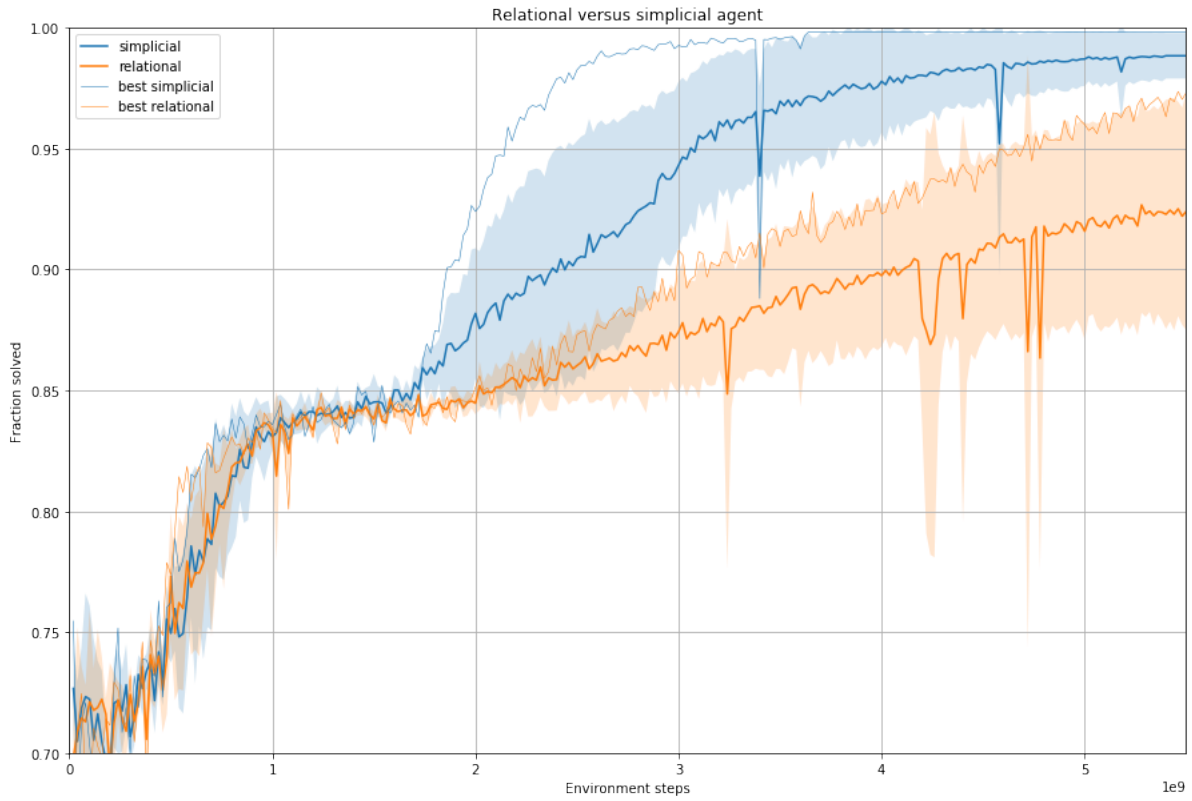


Figure 3: Training curve of mean relational and simplicial agents on bridge BoxWorld. Shown are the mean and standard deviation of four runs of each agent.

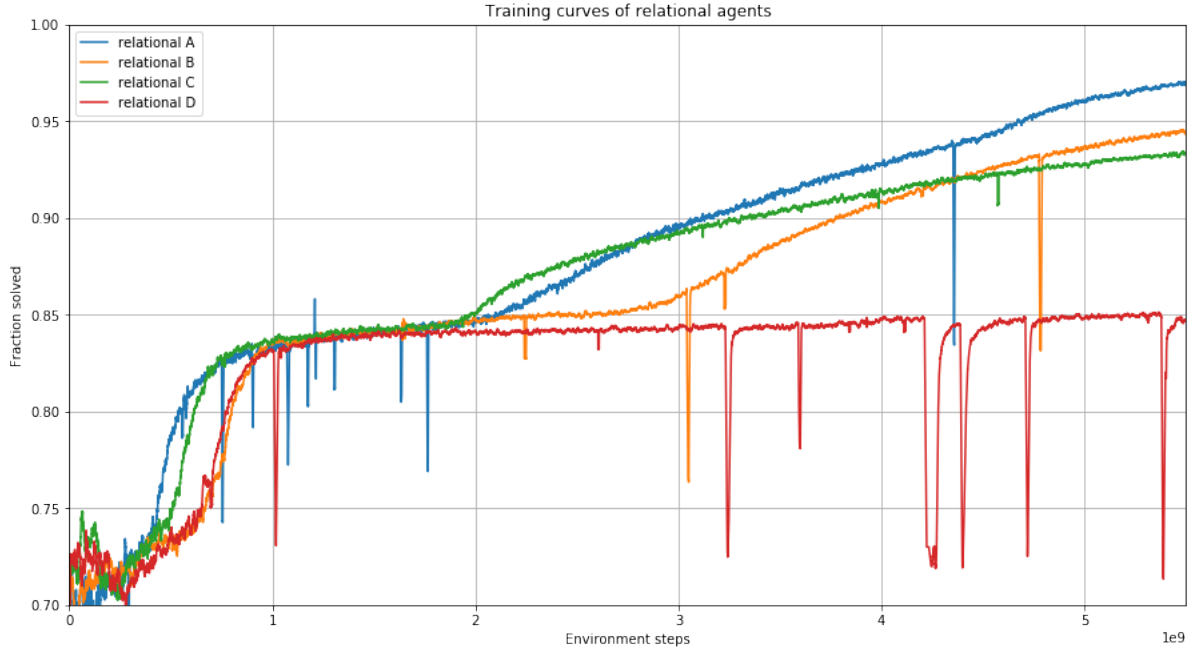


Figure 4: Training curves for the relational agent on bridge BoxWorld.

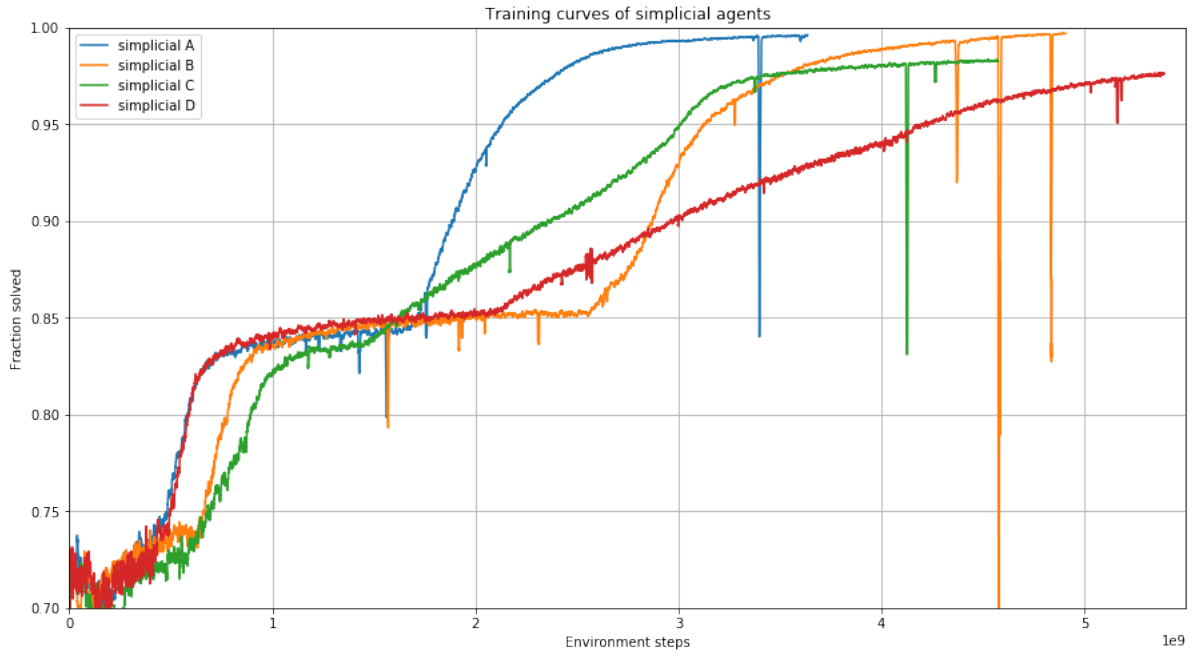


Figure 5: Training curves for the simplicial agent on bridge BoxWorld.

have chosen not to employ an episode horizon. Fortunately, the relational agent performs well even without a curriculum on the original BoxWorld, as our results show.

**Remark 5.2.** Experiments were conducted either on the Google Cloud Platform with a single head node with 12 virtual CPUs and one NVIDIA Tesla P100 GPU and 192 additional virtual CPUs spread over two pre-emptible worker nodes, or on the University of Melbourne Nectar research cloud with a single head node with 12 virtual CPUs and two NVIDIA Tesla K80 GPUs, and 222 worker virtual CPUs.

## 6 Analysis

We analyse the simplicial agent, with two main goals: firstly, to establish that the agent has actually learned to use the 2-simplicial attention, and secondly to examine the hypothesis that the agent has learned a form of logical reasoning. The results of our analysis are positive in the first case but inconclusive in the second: while the agent has clearly learned to use both the 1-simplicial and 2-simplicial attention, we are unable to identify the structure in the attention as a homomorphic image of a logically correct explicit strategy, and so we leave as an open question whether the agent is performing logical reasoning according to the standard elaborated in Appendix B.

It will be convenient to organise episodes of bridge BoxWorld by their *puzzle type*, which is the tuple  $(a, b, c)$  where  $1 \leq a \leq 3$  is the solution length,  $1 \leq b \leq a$  is the *bridge source* and  $a + 1 \leq c \leq 2a$  is the *bridge target*, with indices increasing with the distance from the gem. For example, the episode in Figure 2 has puzzle type  $(3, 2, 5)$ . Throughout this section *simplicial agent* means simplicial agent A of Figure 5.

### 6.1 Attention

We provide a preliminary analysis of the attention of the trained simplicial agent, with an aim to answer the following questions: which standard entities attend to which other standard entities? What do the virtual entities attend to? Is the 2-simplicial attention being used? Our answers are anecdotal, based on examining visualisations of rollouts; we leave a more systematic investigation of the agent’s strategy to future work.

The analysis of the agent’s attention is complicated by the fact that our  $2 \times 2$  convolutional layers (of which there are two) are not padded, so the number of entities processed by the Transformer blocks is  $(R - 2)(C - 1)$  where the original game board is  $R \times C$  and there is an extra column for the inventory (here  $R$  is the number of rows). This means there is not a one-to-one correspondence between game board tiles and entities; for example, all the experiments reported in Figure 3 are on a  $7 \times 9$  board, so that there are  $N = 40$  Transformer entities which can be arranged on a  $5 \times 8$  grid (information about this grid is passed to the Transformer blocks via the positional encoding). Nonetheless we found that for trained agents there is a strong relation between a tile in position  $(y, x)$  and the Transformer entity with index  $x + (C - 1)(y - 1) - 1$  for

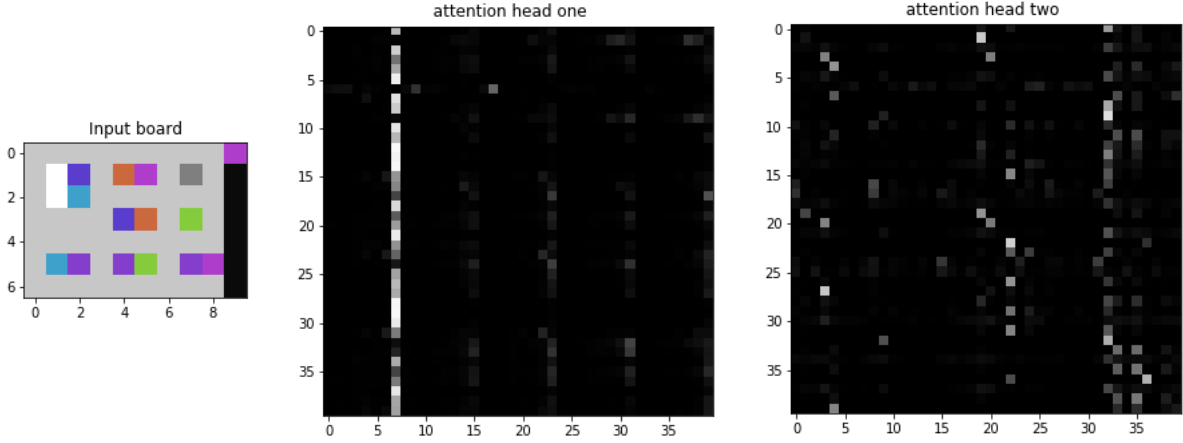


Figure 6: Visualisation of 1-simplicial attention in first Transformer block, between standard entities in heads one and two. The vertical axes on the second and third images are the query index  $0 \leq i \leq 39$ , the horizontal axes are the key index  $0 \leq j \leq 39$ .

$(y, x) \in [1, R - 2] \times [1, C - 1] \subseteq [0, R - 1] \times [0, C]$ . This correspondence is presumed in the following analysis, and in our visualisations.

Across our four trained simplicial agents, the roles of the virtual entities and heads vary: the following comments are all in the context of the best simplicial agent (simplicial agent A of Figure 5) but we observe similar patterns in the other trials.

### 6.1.1 1-simplicial attention of standard entities

The standard entities are now indexed by  $0 \leq i \leq 39$  and virtual entities by  $i = 40, 41$ . In the first iteration of the 2-simplicial Transformer block, the first 1-simplicial head appears to propagate information about the inventory. At the beginning of an episode the attention of each standard entity is distributed between entities 7, 15, 23, 31 (the entities in the rightmost column), it concentrates sharply on 7 (the entity closest to the first inventory slot) after the acquisition of the first loose key, and sharply on 7, 15 after the acquisition of the second loose key. The second 1-simplicial head seems to acquire the meaning described in [69], where tiles of the same colour attend to one another. A typical example is shown in Figure 6. The video of this episode is available online [15].

### 6.1.2 2-simplicial attention

The standard entities are updated using 2-simplices in the first iteration of the 2-simplicial Transformer block, but this is not interesting as initially the virtual entities are learned embedding vectors, containing no information about the current episode. So we restrict our analysis to the 2-simplicial attention in the *second* iteration of the Transformer block. In brief, we observe that the agent has learned to use the 2-simplicial attention to direct

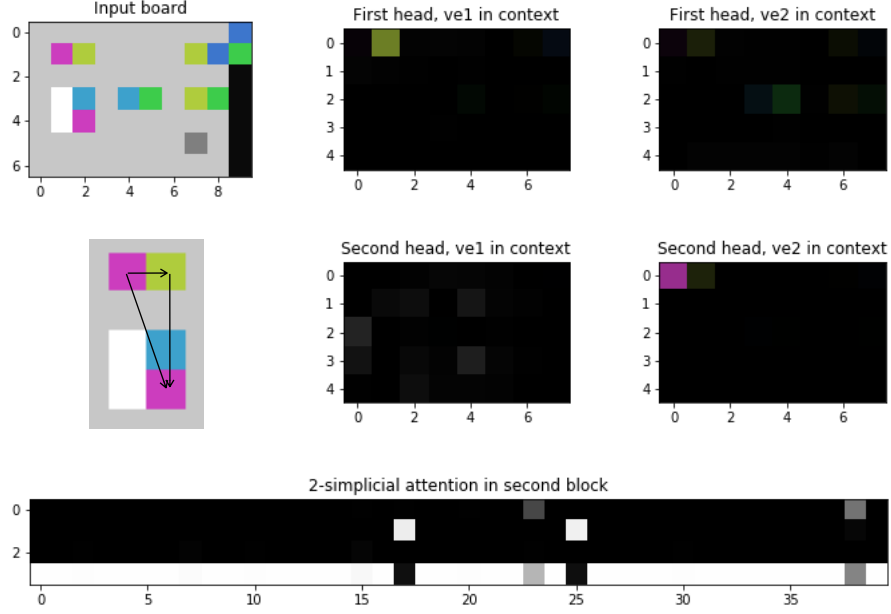


Figure 7: The 1-simplicial attention of the virtual entities in the first iteration (first and second row, second and third column) and 2-simplicial attention in the second iteration, in step 18 of an episode of puzzle type  $(3, 2, 5)$ . Entity 17 is the top lock on the Gem, 25 is the bottom lock on the Gem, 39 is the player. Shown is a 2-simplex with query entity 25. In the visualisations of the 1-simplicial attention, the rows are query entities  $i$  and the columns are key entities  $j$ . In the visualisation of the 2-simplicial attention, the columns are query entities  $i$  and rows are key entity pairs  $(j, k)$  in lexicographic order  $(1, 1), (1, 2), (2, 1), (2, 2)$ .

tensor products of value vectors to specific query entities. In a typical timestep most query entities  $i$  attend strongly to a common pair  $(j, k)$  (which is  $(2, 2)$  in Figures 7 and 9 and  $(2, 1)$  in Figure 8), and we refer to this attention as *generic*. The top and bottom locks on the Gem, the player, and the entities 7, 15 associated to the inventory are often observed to have a non-generic 2-simplicial attention, and some of the relevant 2-simplices are drawn in the aforementioned figures.

To give more details we must first examine the content of the virtual entities after the first iteration, which is a function of the 1-simplicial attention of the virtual entities in the first iteration. In Figures 7, 8, 9 we show these attention distributions multiplied by the pixels in the region  $[1, R - 2] \times [1, C - 1]$  of the original board, in the second and third columns of the second and third rows.<sup>4</sup> Let  $f_1 = e_{40}$  and  $f_2 = e_{41}$  denote the initial

<sup>4</sup>For visibility in print the 1-simplicial attention of the virtual entities in these figures has been sharpened, by multiplying the logits by 2. The 2-simplicial attention and 1-simplicial attention of standard entities have not been sharpened. In this connection, we remark that in Figure 7 there is one entity whose unsharpened attention coefficient for the first virtual entity in the first head is more than one standard

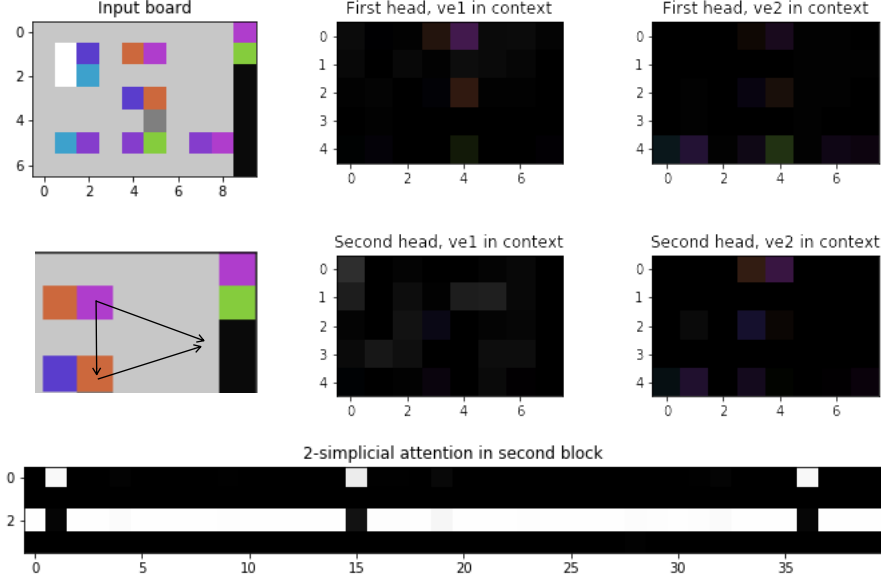


Figure 8: Visualisation of the 2-simplicial attention in the second Transformer block in step 13 of an episode of puzzle type (3,3,5). Entity 1 is the top lock on the Gem, 15 is associated with the inventory, 36 is the lock directly below the player. Shown is a 2-simplex with target 15.

representations of the first and second virtual entities, before the first iteration. We use the index  $z \in \{1, 2\}$  to stand for a virtual entity. In the first iteration the representations are updated by (19) to

$$f'_z = \text{LayerNorm} \left( g_\theta \left[ \left\{ \sum_{\alpha} a_{\alpha}^z v_{\alpha} \right\} \oplus \left\{ \sum_{\alpha} b_{\alpha}^z v_{\alpha} \right\} \right] + f_z \right) \quad (23)$$

where the sum is over all entities  $\alpha$ , the  $a_{\alpha}^z$  are the attention coefficients of the first 1-simplicial head and the coefficients  $b_{\alpha}^z$  are the attention of the second 1-simplicial head. Writing  $\mathbf{0}_1, \mathbf{0}_2$  for the zero vector in  $H_1^1, H_2^1$  respectively, this can be written as

$$f'_z = \text{LayerNorm} \left( g_\theta \left[ \sum_{\alpha} a_{\alpha}^z (v_{\alpha} \oplus \mathbf{0}_2) + \sum_{\alpha} b_{\alpha}^z (\mathbf{0}_1 \oplus v_{\alpha}) \right] + f_z \right). \quad (24)$$

For a query entity  $i$  the vector propagated by the 2-simplicial part of the second iteration has the following terms, where  $\tilde{B} = B \circ (W^U \otimes W^U)$

$$A_{1,1}^i \tilde{B}(f'_1 \otimes f'_1) + A_{1,2}^i \tilde{B}(f'_1 \otimes f'_2) + A_{2,1}^i \tilde{B}(f'_2 \otimes f'_1) + A_{2,2}^i \tilde{B}(f'_2 \otimes f'_2). \quad (25)$$

Here  $A_{j,k}^i$  is the 2-simplicial attention with logits  $\langle p_i, l_j^1, l_k^2 \rangle$  associated to  $(i, j, k)$ .

---

deviation above the mean, and there are two such entities for the second virtual entity and second head.

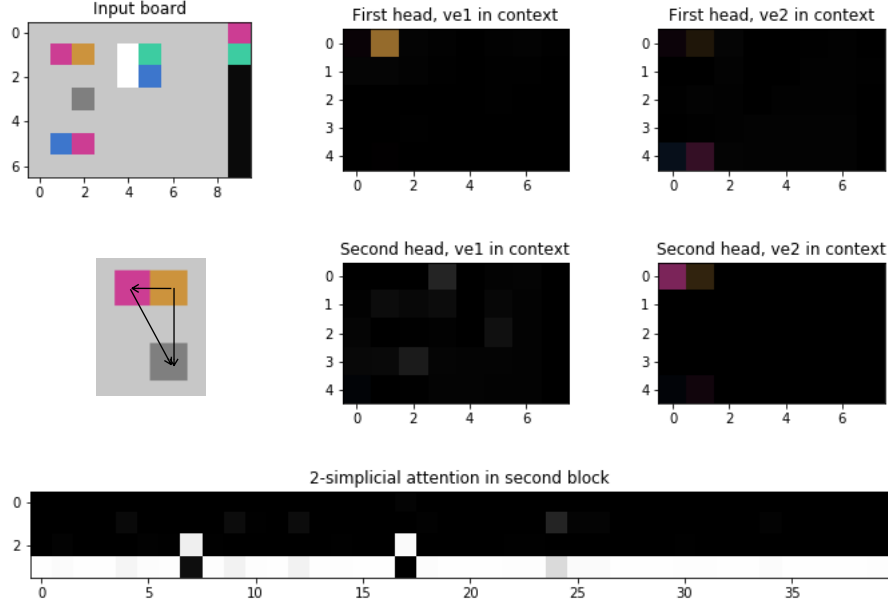


Figure 9: Visualisation of the 2-simplicial attention in the second Transformer block in step 29 of an episode of puzzle type (3, 3, 5). Entity 7 is associated with the inventory, 17 is the player. Shown is a 2-simplex with target 17.

The tuple  $(A_{1,1}^i, A_{1,2}^i, A_{2,1}^i, A_{2,2}^i)$  is the  $i$ th column in our visualisations of the 2-simplicial attention, so in the situation of Figure 7 with  $i = 25$  we have  $A_{1,2}^{25} \approx 1$  and hence the output of the 2-simplicial head used to update the entity representation of the bottom lock on the Gem is approximately  $\tilde{B}(f'_1 \otimes f'_2)$ . If we ignore the layer normalisation, feed-forward network and skip connection in (24) then  $f'_1 \approx v_1 \oplus \mathbf{0}_2$  and  $f'_2 \approx \mathbf{0}_1 \oplus v_0$  so that the output of the 2-simplicial head with target  $i = 25$  is approximately

$$\tilde{B}((v_1 \oplus \mathbf{0}_2) \otimes (\mathbf{0}_1 \oplus v_0)). \quad (26)$$

Following Boole [9] and Girard [25] it is natural to read the “product” (26) as a conjunction (consider together the entity 1 and the entity 0) and the sum in (25) as a disjunction. An additional layer normalisation is applied to this vector, and the result is concatenated with the incoming information for entity 25 from the 1-simplicial attention, before all of this is passed through (17) to form  $e'_{25}$ .

Given that the output of the 2-simplicial head is the only nontrivial difference between the simplicial and relational agent (with a transformer depth of two, the first 2-simplicial Transformer block only updates the standard entities with information from embedding vectors) the performance differences reported in Figure 3 suggest that this output is informative about avoiding bridges.

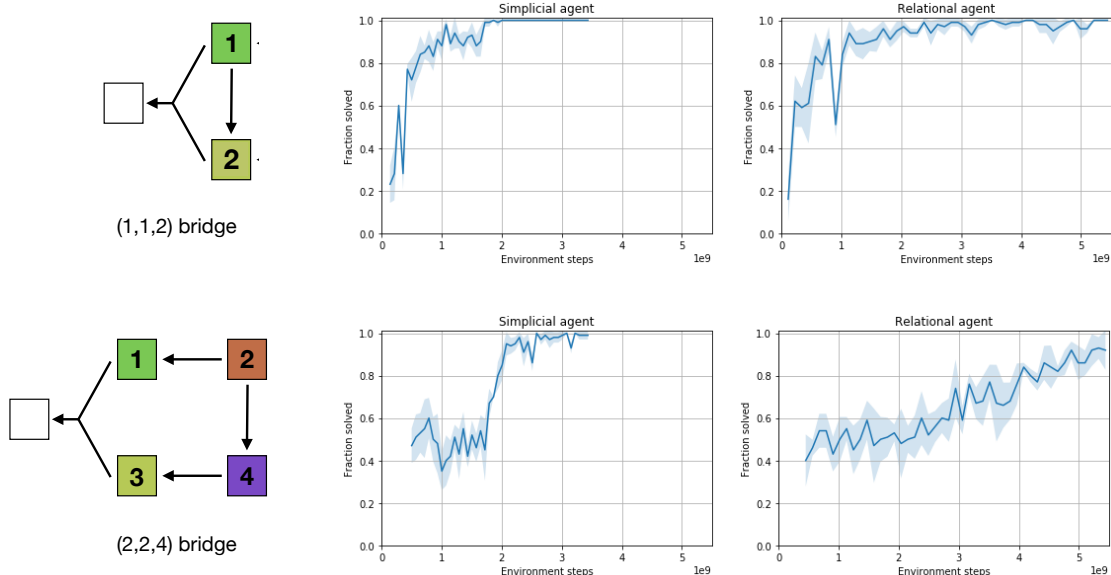


Figure 10: Simplicial and relational agent win rate on puzzle types  $(1, 1, 2)$ ,  $(2, 2, 4)$ .

## 6.2 The plateau

In the training curves of the agents of Figure 4 and Figure 5 we observe a common plateau at a win rate of 0.85. In Figure 10 we show the per-puzzle win rate of simplicial agent A and relational agent A, on  $(1, 1, 2)$  puzzles. These graphs make clear that the transition of both agents to the plateau at 0.85 is explained by solving the  $(1, 1, 2)$  type (and to a lesser degree by progress on all puzzle types with  $b = 1$ ). In Figure 10 and Figure 11 we give the per-puzzle win rates for a small sample of other puzzle types. Shown are the mean and standard deviation of 100 runs across various checkpoints of simplicial agent A and relational agent A.

## 7 Discussion

Motivated by the idea that abstract reasoning in humans is grounded in structural representations that are adapted from those evolved for spatial reasoning, we have presented a simplicial inductive bias. We have shown that in the context of a deep reinforcement learning environment with nontrivial logical structure, this bias is superior to a purely relational inductive bias. In this concluding section we briefly address some of the limitations of our work, and future directions.

**Limitations.** Our experiments involve only a small number of virtual entities, and a small number of iterations of the Transformer block: it is possible that for large numbers of virtual entities and iterations, our choices of layer normalisation are not optimal. Our



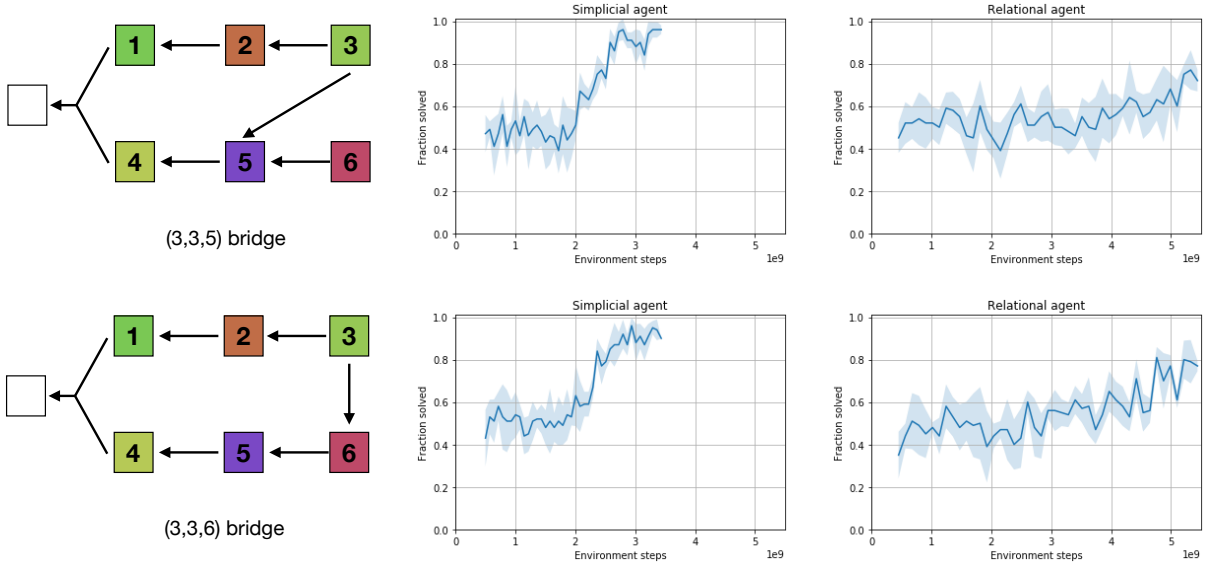


Figure 11: Simplicial and relational agent win rate on puzzle types (3, 3, 5), (3, 3, 6).

aim was to test the viability of the simplicial Transformer starting with the minimal configuration, so we have also not tested multiple heads of 2-simplicial attention.

Deep reinforcement learning is notorious for poor reproducibility [31], and in an attempt to follow the emerging best practices we are releasing our agent and environment code, trained agent weights, and training notebooks [15].

**Future directions.** It is clear using the general formulas for the unsigned scalar product how to define an  $n$ -simplicial Transformer block, and this is arguably an idiomatic expression in the context of deep learning of the linear logic semantics of the  $\otimes$  connective. It would be interesting to extend this to include other connectives, in environments encoding a larger fragment of linear logic proofs. However, at present this seems out of reach because the  $O(N^2)$  complexity makes scaling to much larger environments impractical. We hope that some of the scaling work being done in the Transformer literature can be adapted to the simplicial Transformer; see for example [12].

## A Clifford algebra

The volume of an  $n$ -simplex in  $\mathbb{R}^n$  with vertices at  $0, v_1, \dots, v_n$  is

$$\text{Vol}_n = \left| \frac{1}{n!} \det(v_1, \dots, v_n) \right|$$

which is  $\frac{1}{n!}$  times the volume of the  $n$ -dimensional parallelotope which shares  $n$  edges with the  $n$ -simplex. In our applications the space of representations  $H$  is high dimensional,

but we wish to speak of the volume of  $k$ -simplices for  $k < \dim(H)$  and use those volumes to define the coefficients of our simplicial attention. The theory of Clifford algebras [32] is one appropriate framework for such calculations.

Let  $H$  be an inner product space with pairing  $(v, w) \mapsto v \cdot w$ . The Clifford algebra  $\text{Cl}(H)$  is the associative unital  $\mathbb{R}$ -algebra generated by the vectors  $v \in H$  with relations

$$vw + wv = 2(v \cdot w) \cdot 1.$$

The canonical  $k$ -linear map  $H \rightarrow \text{Cl}(H)$  is injective, and since  $v^2 = \|v\|^2 \cdot 1$  in  $\text{Cl}(H)$ , any nonzero vector  $v \in H$  is a unit in the Clifford algebra. While as an algebra  $\text{Cl}(H)$  is only  $\mathbb{Z}_2$ -graded, there is nonetheless a  $\mathbb{Z}$ -grading of the underlying vector space which can be defined as follows: let  $\{e_i\}_{i=1}^n$  be an orthonormal basis of  $H$ , then the set

$$\mathcal{B} = \{e_{i_1} \cdots e_{i_m}\}_{i_1 < \cdots < i_m}$$

is a basis for  $\text{Cl}(H)$ , with  $m$  ranging over the set  $\{0, \dots, n\}$ . If we assign the basis element  $e_{i_1} \cdots e_{i_m}$  the degree  $m$  then this determines a  $\mathbb{Z}$ -grading  $[-]_k$  of the Clifford algebra, which is easily checked to be independent of the choice of basis.

**Definition A.1.**  $[A]_k$  denotes the homogeneous component of  $A \in \text{Cl}(H)$  of degree  $k$ .

**Example A.2.** Given  $a, b, c \in H$  we have  $[ab]_0 = a \cdot b$ ,  $[ab]_2 = a \wedge b$  and

$$[abc]_1 = (a \cdot b)c - (a \cdot c)b + (b \cdot c)a, \quad [abc]_3 = a \wedge b \wedge c. \quad (27)$$

There is an operation on elements of the Clifford algebra called *reversion* in geometric algebra [32, p.45] which arises as follows: the opposite algebra  $\text{Cl}(H)^{\text{op}}$  admits a  $k$ -linear map  $j : H \rightarrow \text{Cl}(H)^{\text{op}}$  with  $j(v) = v$  which satisfies  $j(v)j(w) + j(w)j(v) = 2(v \cdot w) \cdot 1$ , and so by the universal property there is a unique morphism of algebras

$$(-)^\dagger : \text{Cl}(H) \rightarrow \text{Cl}(H)^{\text{op}}$$

which restricts to the identity on  $H$ . Note  $(v_1 \cdots v_k)^\dagger = v_k^\dagger \cdots v_1^\dagger$  for  $v_1, \dots, v_k \in H$  and  $(-)^\dagger$  is homogeneous of degree zero with respect to the  $\mathbb{Z}$ -grading. Using this operation we can define the magnitude [32, p.46] of any element of the Clifford algebra.

**Definition A.3.** The *magnitude* of  $A \in \text{Cl}(H)$  is  $|A| = \sqrt{[A^\dagger A]_0}$ .

For vectors  $v_1, \dots, v_k \in H$ ,

$$|v_1 \cdots v_k|^2 = [v_k \cdots v_1 v_1 \cdots v_k]_0 = \|v_1\|^2 \cdots \|v_k\|^2 \quad (28)$$

and in particular for  $v \in H$  we have  $|v| = \|v\|$ .

**Lemma A.4.** Set  $n = \dim(H)$ . Then for  $A \in \text{Cl}(H)$  we have

$$|A|^2 = \sum_{i=0}^n |[A]_i|^2.$$

*Proof.* See [32, (1.33)]. □

**Example A.5.** For  $a, b, c \in H$  the lemma gives

$$\|a\|^2 \|b\|^2 \|c\|^2 = |[abc]_1|^2 + |[abc]_3|^2 = \|(a \cdot b)c - (a \cdot c)b + (b \cdot c)a\|^2 + |a \wedge b \wedge c|^2$$

and hence

$$\|(a \cdot b)c - (a \cdot c)b + (b \cdot c)a\|^2 = \|a\|^2 \|b\|^2 \|c\|^2 - |a \wedge b \wedge c|^2.$$

**Remark A.6.** Given vectors  $v_1, \dots, v_k \in H$  the wedge product  $v_1 \wedge \dots \wedge v_k$  is an element in the exterior algebra  $\bigwedge H$ . Using the chosen orthogonal basis  $\mathcal{B}$  we can identify the underlying vector space of  $\text{Cl}(H)$  with  $\bigwedge H$  and using this identification (set  $v_i = \sum_j \lambda_{ij} e_j$ )

$$\begin{aligned} [v_1 \cdots v_k]_k &= \left[ \left( \sum_{j_1=1}^n \lambda_{1j_1} e_{j_1} \right) \cdots \left( \sum_{j_k=1}^n \lambda_{kj_k} e_{j_k} \right) \right]_k \\ &= \sum_{j_1, \dots, j_k} \lambda_{1j_1} \cdots \lambda_{kj_k} [e_{j_1} \cdots e_{j_k}]_k \\ &= \sum_{\substack{1 \leq j_1 < \dots < j_k \leq n \\ \sigma \in S_k}} \lambda_{1j_{\sigma(1)}} \cdots \lambda_{kj_{\sigma(k)}} [e_{j_{\sigma(1)}} \cdots e_{j_{\sigma(k)}}]_k \\ &= \sum_{\substack{1 \leq j_1 < \dots < j_k \leq n \\ \sigma \in S_k}} (-1)^{|\sigma|} \lambda_{1j_{\sigma(1)}} \cdots \lambda_{kj_{\sigma(k)}} e_{j_1} \cdots e_{j_k} \\ &= v_1 \wedge \cdots \wedge v_k \end{aligned}$$

where  $S_k$  is the permutation group on  $k$  letters. That is, the top degree piece of  $v_1 \cdots v_k$  in  $\text{Cl}(H)$  is always the wedge product. It is then easy to check that the squared magnitude of this wedge product is

$$|[v_1 \cdots v_k]_k|^2 = \sum_{1 \leq j_1 < \dots < j_k \leq n} \left( \sum_{\sigma \in S_k} \lambda_{1j_{\sigma(1)}} \cdots \lambda_{kj_{\sigma(k)}} \right)^2. \quad (29)$$

The term in the innermost bracket is the determinant of the  $k \times k$  submatrix with columns  $\mathbf{j} = (j_1, \dots, j_k)$  and in the special case where  $k = n = \dim(H)$  we see that the squared magnitude is just the square of the determinant of the matrix  $(\lambda_{ij})_{1 \leq i, j \leq n}$ .

The wedge product of  $k$ -vectors in  $H$  can be thought of as an oriented  $k$ -simplex, and the magnitude of this wedge product in the Clifford algebra computes the volume.

**Definition A.7.** The *volume* of a  $k$ -simplex in  $H$  with vertices  $0, v_1, \dots, v_k$  is

$$\text{Vol}_k = \frac{1}{k!} |[v_1 \cdots v_k]_k|. \quad (30)$$

**Definition A.8.** Given  $v_1, \dots, v_k \in H$  the  $k$ -fold unsigned scalar product is

$$\langle v_1, \dots, v_k \rangle = \sqrt{\sum_{i=0}^{k-1} |[v_1 \cdots v_k]_i|^2}. \quad (31)$$

By Lemma A.4 and (28) we have

$$\langle v_1, \dots, v_k \rangle^2 = \|v_1\|^2 \cdots \|v_k\|^2 - (k!)^2 \text{Vol}_k^2 \quad (32)$$

which gives the desired generalisation of (12), (13).

**Example A.9.** For  $k = 2$  the unsigned scalar product is the absolute value of the dot product,  $\langle a, b \rangle = |a \cdot b|$ . For  $k = 3$  we obtain the formulas of Definition 2.5, from which it is easy to check that

$$\langle a, b, c \rangle = \|a\| \|b\| \|c\| \sqrt{\cos^2 \theta_{ab} + \cos^2 \theta_{bc} + \cos^2 \theta_{ac} - 2 \cos \theta_{ab} \cos \theta_{ac} \cos \theta_{bc}} \quad (33)$$

where  $\theta_{ac}, \theta_{ab}, \theta_{bc}$  are the angles between  $a, b, c$ . The geometry of the three-dimensional case is more familiar: if  $\dim(H) = 3$  then  $|[abc]_3|$  is the absolute value of the determinant by (29), so that  $\text{Vol}_3 = \frac{1}{6}|a \cdot (b \times c)|$  is the usual formula for the volume of the 3-simplex. Recall that  $|a \cdot (b \times c)| = \|a\| \|b\| \|c\| |\sin(\theta_{bc})| |\cos(\phi)|$  where  $\phi$  is the angle between the cross product  $a$  and  $b \times c$ . Hence, in this case the scalar triple product is

$$\langle a, b, c \rangle = \|a\| \|b\| \|c\| \sqrt{1 - \sin^2(\theta_{ab}) \cos^2(\phi)}. \quad (34)$$

With these formulas in mind the geometric content of the following lemma is clear:

**Lemma A.10.** Let  $v_1, \dots, v_k \in H$ . Then

- (i)  $0 \leq \langle v_1, \dots, v_k \rangle \leq \|v_1\| \cdots \|v_k\|$ .
- (ii) If the  $v_i$  are all pairwise orthogonal then  $\langle v_1, \dots, v_k \rangle = 0$ .
- (iii) The set  $\{v_1, \dots, v_k\}$  is linearly dependent if and only if  $\langle v_1, \dots, v_k \rangle = \|v_1\| \cdots \|v_k\|$ .
- (iv) For any  $\sigma \in S_k$  we have  $\langle v_1, \dots, v_k \rangle = \langle v_{\sigma(1)}, \dots, v_{\sigma(k)} \rangle$ .
- (v) For  $\lambda_1, \dots, \lambda_k \in \mathbb{R}$ , we have

$$\langle \lambda_1 v_1, \dots, \lambda_k v_k \rangle = |\lambda_1| \cdots |\lambda_k| \langle v_1, \dots, v_k \rangle.$$

*Proof.* (i) is obvious from (31), (32). For (ii) note that

$$v_1 \wedge \cdots \wedge v_k = \frac{1}{k!} \sum_{\sigma \in S_k} (-1)^{|\sigma|} v_{\sigma(1)} \cdots v_{\sigma(k)} \quad (35)$$

and hence if the  $v_i$  are pairwise orthogonal, and therefore anticommute in  $\text{Cl}(H)$ , we have  $v_1 \wedge \cdots \wedge v_k = v_1 \cdots v_k$ . But the left hand side is homogeneous of degree  $k$ , so this means that  $[v_1 \cdots v_k]_i = 0$  for  $i < k$  and hence that  $\langle v_1, \dots, v_k \rangle = 0$ . The property (iii) is a standard property of wedge products. Finally, (iv) is clear from (32) and (v) is clear since  $|\lambda A| = |\lambda||A|$  for any  $A \in \text{Cl}(H)$ .  $\square$

For more on simplicial methods in the context of geometric algebra see [59, 42].

## B Logic and reinforcement learning

It is no simple matter to define *logical reasoning* nor to recognise when an agent (be it an animal or a deep reinforcement learning agent) is employing such reasoning [44, 5]. We therefore begin by returning to Aristotle, who viewed logic as the study of general patterns by which one could distinguish valid and invalid forms of philosophical argumentation; this study having as its purpose the production of *strategies* for winning such argumentation games [2, 58, 61]. In this view, logic involves

- **two players** with one asserting the truth of a proposition and attempting to defend it, and the latter asserting its falsehood and attempting to refute it, and an
- **observer** attempting to learn the general patterns which are predictive of which of the two players will win such a game given some intermediate state.

Suppose we observe over a series of games<sup>5</sup> that a player is following an explicit strategy which has been distilled from general patterns observed in a large distribution of games, and that by following this strategy they almost always win. A component of that explicit strategy can be thought of as logical reasoning to the degree that it consists of rules that are independent of the particulars of the game [2, §11.25]. The problem of recognising logical reasoning in behaviour is therefore twofold: the strategy employed by a player is typically *implicit*, and even if we can recognise explicit components of the strategy, in practice there is not always a clear way to decide which rules are domain-specific.

In mathematical logic the idea of argumentation games has been developed into a theory of *mathematical proof as strategy* in the game semantics of linear logic [35] where one player (the *prover*) asserts a proposition  $G$  and the other player (the *refuter*) interrogates

---

<sup>5</sup>We cannot infer that a behaviour constitutes logical reasoning if we only observe it over the course of a single game. For example, while it may appear that a human proving a statement in mathematics by correctly applying a set of deduction rules is engaged in logical reasoning, this appearance may be false, for if we were to observe one thousand attempts to prove a sample of similar propositions, and in only one attempt was the human able to correctly apply the deduction rules, we would have to retract our characterisation of the behaviour as logical reasoning. The concept is also empty if we insist that it applies only if in *every* such attempt the deduction rules are correctly applied, because human mathematicians make mistakes.

this assertion.<sup>6</sup> Consider a reinforcement learning problem [63] in which the deterministic environment encodes  $G$  together with a multiset of hypotheses  $\Gamma$  which are sufficient to prove  $G$ . Such a pair is called a *sequent* and is denoted  $\Gamma \vdash G$ . The goal of the agent (in the role of prover) is to synthesise a proof of  $G$  from  $\Gamma$  through a series of actions. The environment (in the role of refuter) delivers a positive reward if the agent succeeds, and a negative reward if the agent’s actions indicate a commitment to a line of proof which cannot possibly succeed. Consider a deep reinforcement learning agent with a policy network parametrised by a vector of weights  $\mathbf{w} \in \mathbb{R}^D$  and a sequence of full-episode rollouts of this policy in the environment, each of which either ends with the agent constructing a proof (prover wins) or failing to construct a proof (refuter wins) with the sequent  $\Gamma \vdash G$  being randomly sampled in each episode. Viewing these episodes as instances of an argumentation game, the goal of Aristotle’s observer is to learn from this data to predict, given an intermediate state of some particular episode, which actions by the prover will lead to success (proof) or failure (refutation). As the reward is correlated with success and failure in this sense, the goal of the observer may be identified with the training objective of the action-value network underlying the agent’s policy, and we may identify the triple *player, opponent, observer* with the triple *agent, environment* and *optimisation process*. If this process succeeds, so that the trained agent wins in almost every episode, then by definition the weights  $\mathbf{w}$  are an *implicit strategy* for proving sequents  $\Gamma \vdash G$ .

This leads to the question: is the deep reinforcement learning agent parametrised by  $\mathbf{w}$  performing logical reasoning? We would have no reason to deny that logical reasoning is present if we were to find, in the weights  $\mathbf{w}$  and dynamics of the agent’s network, an isomorphic image of an explicit strategy that we recognise as logically correct. In general, however, it seems more useful to ask *to what degree* the behaviour is governed by logical reasoning, and thus to what extent we can identify an approximate *homomorphic* image in the weights and dynamics of a logically correct explicit strategy. Ultimately this should be automated using “logic probes” along the lines of recent developments in neural network probes [1, 38, 48, 56, 57].

**Remark B.1.** In the context of bridge BoxWorld, here is a strategy that would qualify as logical reasoning by the above standard: call a pair of boxes  $\alpha, \beta$  a *source* if they have the same lock colour but distinct key colours, and a *sink* if they have the same key colour but distinct lock colours. If  $\alpha, \beta$  is a source or a sink then either  $\alpha$  is the bridge or  $\beta$  is the bridge. Therefore, if you observe both a source and a sink then you can locate the bridge. This strategy contains perceptual components (learning to recognise sources and sinks) and components that qualify as logical reasoning (using the combination of a source and a sink to identify the bridge).

---

<sup>6</sup>It is possible for the prover to win such an argument without possessing a proof (for instance if  $G$  is the disjunct of propositions  $A, B$  and the refuter demands a proof of  $A$  in a situation where the prover knows a proof of  $A$  but not of  $B$ ) but the only strategy guaranteed to win is to play according to a proof.

## B.1 Strategies and proof trees

We explain the correspondence between agent behaviour in bridge BoxWorld and proofs in linear logic. For an introduction to linear logic tailored to the setting of games see [45, Ch.2]. Recall that to each colour  $c$  we have associated a proposition  $C$  which can be read as “the key of colour  $c$  is obtainable”. If a box  $\beta$  appears in an episode of bridge BoxWorld (this includes loose keys and the box with the Gem) then we assume given a proof  $\pi^\beta$  of a sequent associated to the box by the following rules: the sequent  $X_\beta \vdash Y_\beta$  associated to a loose key of colour  $c$  is  $\vdash C$ , the sequent associated to an ordinary box with a lock of colour  $c$  and containing a key of colour  $c'$  is  $C \vdash C'$  and the sequent associated to a multiple lock on the Gem, with key colours  $c, c'$  is  $C \otimes C' \vdash \mathbb{G}$ . In the following we identify the box  $\beta$  with its associated sequent, and write for example  $\pi^{\vdash C}$  for the chosen proof associated to the loose key of colour  $c$ . The set of premises (or axioms) in an episode of bridge BoxWorld is the multiset  $\Gamma$  of proofs  $\pi^\beta$  as  $\beta$  ranges over all boxes.

**Definition B.2.** Given a formula  $A$  (thought of as representing the contents of the inventory) and a box  $\beta$  we define the proof  $\pi_A^\beta$  to be

$$\begin{array}{c} \pi^\beta \\ \vdots \\ \frac{A \vdash A \quad X_\beta \vdash Y_\beta}{A, X_\beta \vdash A \otimes Y_\beta} \otimes R \\ \frac{A \otimes X_\beta \vdash A \otimes Y_\beta}{A \otimes X_\beta \vdash A \otimes Y_\beta} \otimes L \end{array} \quad (36)$$

One can think of this proof as the algorithm which acts to update the contents of the inventory upon opening the box  $\beta$ .

**Example B.3.** Consider the episode of Figure 2 and suppose that the agent follows the upper solution path and then the lower, obtaining the keys in the following order:  $g$  (green),  $o$  (orange),  $g'$  (dark green),  $m$  (magenta),  $p$  (purple) and  $b$  (blue). Then the proof tree whose computational content matches this behaviour is given by:

$$\begin{array}{c} \begin{array}{c} \pi^{\vdash G} \\ \vdots \\ \vdash G \end{array} \quad \begin{array}{c} \pi^{G \vdash O} \\ \vdots \\ G \vdash O \end{array} \quad \begin{array}{c} \pi^{O \vdash G'} \\ \vdots \\ O \vdash G' \end{array} \quad \begin{array}{c} \pi^{\vdash M} \\ \vdots \\ G' \vdash G' \otimes M \end{array} \quad \begin{array}{c} \pi^{M \vdash P} \\ \vdots \\ G' \otimes M \vdash G' \otimes P \end{array} \quad \begin{array}{c} \pi^{P \vdash B} \\ \vdots \\ G' \otimes P \vdash G' \otimes B \end{array} \\ \hline \vdash G \quad \vdash O \quad \vdash G' \quad \vdash G' \otimes M \quad \vdash G' \otimes P \quad \vdash G' \otimes B \end{array} \quad (37)$$

where unlabelled deduction rules are cuts. Cutting this proof tree against the proof  $\pi^{G' \otimes B \vdash \mathbb{G}}$  associated to the final box gives the proof encoding the agent’s strategy.

This example makes clear the general rule for associating a proof tree to an agent’s strategy, as embodied in its behaviour: take the sequence of boxes  $\beta_1, \dots, \beta_N$  opened by the agent together with the state of the inventory  $I_1, \dots, I_N$  at the time of each opening, and cut the corresponding sequence of proofs  $\pi_{I_i}^{\beta_i}$  against one another.

## C Time adjusted performance

In Figure 3 the horizontal axis is environment steps. However, since the simplicial agent has a more complex model, each environment step takes longer to execute and the gradient descent steps are slower. In a typical experiment run on the GCP configuration in Remark 5.2, the training throughput of the relational agent is  $1.9 \times 10^4$  environment frames per second (FPS) and that of the simplicial agent is  $1.4 \times 10^4$  FPS. The relative performance gap decreases as the GPU memory and the number of IMPALA workers are increased, and this is consistent with the fact that the primary performance difference appears to be the time taken to compute the gradients (35ms vs 80ms). In Figure 12 we give the time-adjusted performance of the simplicial agent (the graph for the relational agent is as before) where the  $x$ -axis of the graph of the simplicial agent is scaled by  $1.9/1.4$ .

In principle there is no reason for a significant performance mismatch: the 2-simplicial attention can be run in parallel to the ordinary attention (perhaps with two iterations of the 1-simplicial attention per iteration of the 2-simplicial attention) so that with better engineering it should be possible to reduce this gap.

## D Comparison to NTM

The Transformer block and descendents such as the Universal Transformer [17] can be viewed as general units for computing with learned representations; in this sense they have a similar conceptual role to the Neural Turing Machine (NTM) [28] and Differentiable Neural Computer [29]. As pointed out in [17, §4] one can view the Transformer as a block of parallel RNNs (one for each entity) which update their hidden states at each time step by attending to the sequence of hidden states of the other RNNs at the previous step. We expand on those remarks here in order to explain the connection between the 2-simplicial Transformer and earlier work in the NLP literature, which is written in terms of RNNs.

We consider a NTM with content-based addressing only and no sharpening. The core of the NTM is an RNN controller with update rule

$$h' = \text{ReLU}(M + Wh + Ux + b) \quad (38)$$

where  $W, U, b$  are weight matrices,  $x$  is the current input symbol,  $h$  is the previous hidden state,  $h'$  is the next hidden state and  $M$  is the output of the *memory read head*

$$M = \sum_{j=1}^N \text{softmax}(K[q, M_1], \dots, K[q, M_N])_j M_j \quad (39)$$



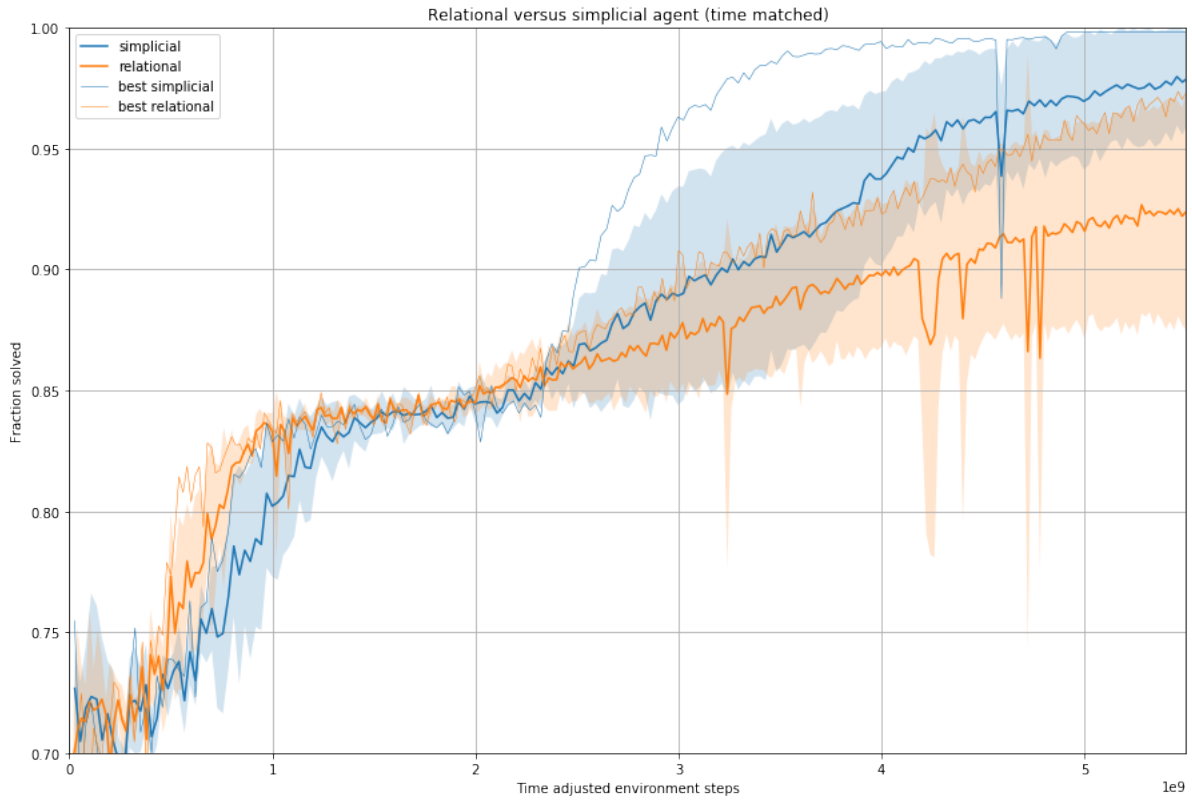


Figure 12: Training curve of mean relational and simplicial agents on bridge BoxWorld, with time-adjusted  $x$ -axis for the simplicial agent.

where there are  $N$  memory slots containing  $M_1, \dots, M_N$ ,  $q$  is a query generated from the hidden state of the RNN by a weight matrix  $q = Zh$ , and  $K[u, v] = (u \cdot v) / (\|u\| \|v\|)$ . We omit the mechanism for writing to the memory here, since it is less obvious how that relates to the Transformer; see [28, §3.2]. Note that while we can view  $M_j$  as the “hidden state” of memory slot  $j$ , the controller’s hidden state and the hidden states of the memory slots play asymmetric roles, since the former is updated with a feedforward network at each time step, while the latter is not.

The Transformer with shared transition functions between layers is analogous to a NTM with this asymmetry removed: there is no longer a separate recurrent controller, and every memory slot is updated with a feedforward network in each timestep. To explain, view the entity representations  $e_1, \dots, e_N$  of the Transformer as the hidden states of  $N$  parallel RNNs. The new representation is

$$e'_i = \text{LayerNorm}(g_\theta(A) + e_i) \quad (40)$$

where the attention term is

$$A = \sum_{j=1}^N \text{softmax}(q_i \cdot k_1, \dots, q_i \cdot k_N) v_j \quad (41)$$

and  $q_i = Ze_i$  is a query vector obtained by a weight matrix from the hidden state, the  $k_j = Ke_j$  are key vectors and  $v_j = Ve_j$  is the value vector. Note that in the Transformer the double role of  $M_j$  in the NTM has been replaced by two separate vectors, the key and value, and the cosine similarity  $K[-, -]$  has been replaced by the dot product.

Having now made the connection between the Transformer and RNNs, we note that the second-order RNN [22, 50, 27, 23] and the similar multiplicative RNN [62, 36] have in common that the update rule for the hidden state of the RNN involves a term  $V(x \otimes h)$  which is a linear function of the tensor product of the current input symbol  $x$  and the current hidden state  $h$ . One way to think of this is that the weight matrix  $V$  maps inputs  $x$  to linear operators on the hidden state. In [60] the update rule contains a term  $V(e_1 \otimes e_2)$  where  $e_1, e_2$  are entity vectors, and this is directly analogous to our construction.

## E Large epsilon RMSProp

As originally presented in [65] the optimisation algorithm RMSProp is a mini-batch version of Rprop, where instead of dividing by a different number in every mini-batch (namely, the absolute value of the gradient) we force this number to be similar for adjacent mini-batches by keeping a moving average of the square of the gradient. In more detail, one step Rprop is computed by the algorithm

$$\begin{aligned} r_i &\leftarrow g_i^2 \\ x_i &\leftarrow x_i - \frac{\kappa g_i}{\sqrt{r_i} + \varepsilon} \end{aligned}$$

where  $\kappa$  is the learning rate,  $x_i$  is a weight,  $g_i$  is the associated gradient and  $\varepsilon$  is a small constant (the TensorFlow default value is  $10^{-10}$ ) added for numerical stability. The idea of Rprop is to update weights using only the *sign* of the gradient: every weight is updated by the same absolute amount  $\kappa$  in each step, with only the sign  $g_i/\sqrt{r_i} = g_i/|g_i|$  of the update varying with  $i$ . The algorithm RMSprop was introduced as a refinement of Rprop:

$$\begin{aligned} r_i &\leftarrow pr_i + (1 - p)g_i^2 \\ x_i &\leftarrow x_i - \frac{\kappa g_i}{\sqrt{r_i + \varepsilon}} \end{aligned}$$

where  $p$  is the *decay rate* (in our experiments the value is 0.99). Clearly Rprop is the  $p \rightarrow 0$  limit of RMSprop. For further background see [26, §8.5.2].

In recent years there has been a trend in the literature towards using RMSprop with large values of the hyperparameter  $\varepsilon$ . For example in [69] RMSprop is used with  $\varepsilon = 0.1$ , which is also one of the range of values in [20, Table D.1] explored by population based training [37]. This “large  $\varepsilon$  RMSprop” seems to have originated in [64, §8]. To understand what large  $\varepsilon$  RMSprop is doing, let us rewrite the algorithm as

$$\begin{aligned} r_i &\leftarrow pr_i + (1 - p)g_i^2 \\ x_i &\leftarrow x_i - \frac{\kappa g_i}{\sqrt{r_i}} \cdot \frac{1}{\sqrt{1 + \varepsilon/r_i}} \\ &= x_i - \frac{\kappa g_i}{\sqrt{r_i}} S\left[\frac{\sqrt{r_i}}{\sqrt{\varepsilon}}\right] \end{aligned}$$

where  $S$  is the sigmoid  $S(u) = u/\sqrt{1 + u^2}$  which asymptotes to 1 as  $u \rightarrow +\infty$  and is well-approximated by the identity function for small  $u$ . We see a new multiplicative factor  $S(\sqrt{r_i}/\sqrt{\varepsilon})$  in the optimisation algorithm. Note that  $\sqrt{r_i}$  is a moving average of  $|g_i|$ . Recall the original purpose of Rprop was to update weights using only the sign of the gradient and the learning rate, namely  $\kappa g_i/\sqrt{r_i}$ . The new  $S$  factor in the above reinserts the size of the gradient, but scaled by the sigmoid to be in the unit interval.

In the limit  $\varepsilon \rightarrow 0$  we squash the outputs of the sigmoid up near 1 and the standard conceptual description of RMSprop applies. But as  $\varepsilon \rightarrow 1$  the sigmoid  $S(\sqrt{r_i})$  has the effect that for large stable gradients we get updates of size  $\kappa$  and for small stable gradients we get updates of the same magnitude as the gradient. In conclusion, large  $\varepsilon$  RMSprop is a form of RMSprop with *smoothed gradient clipping* [26, §10.11.1].

## References

- [1] G. Alain and Y. Bengio, *Understanding intermediate layers using linear classifier probes*, in Proceedings of the International Conference on Learning Representations (ICLR), 2016.

- [2] Aristotle, *Sophistical refutations*, translated by W. A. Pickard-Cambridge, *Complete works of Aristotle, Volume 1: The revised Oxford translation*, J. Barnes (ed.) Princeton University Press, 1984.
- [3] J. Lei Ba, J. R. Kiros and G. E. Hinton, *Layer normalization*, preprint arXiv:1607.06450, 2016.
- [4] D. Bahdanau, K. Cho and Y. Bengio, *Neural machine translation by jointly learning to align and translate*, in Proceedings of the International Conference on Learning Representations (ICLR), 2015.
- [5] D. G. T. Barrett, F. Hill, A. Santoro, A. S. Morcos and T. Lillicrap, *Measuring abstract reasoning in neural networks*, in Proceedings of the International Conference on Machine Learning (ICML), 2018.
- [6] T. E. J. Behrens, T. H. Muller, J. C. R. Whittington, S. Mark, A. B. Baram, K. L. Stachenfeld and Z. Kurth-Nelson, *What is a cognitive map? Organizing knowledge for flexible behavior*, Neuron 100, pp. 490–509, 2018.
- [7] J. L. S. Bellmund, P. Gardenfors, E. I. Moser and C. F. Doeller, *Navigating cognition: Spatial codes for human thinking*, Science 362, 2018.
- [8] J. C. W. Billings, M. Hu, G. Lerda, A. N. Medvedev, F. Mottes, A. Onicas, A. Santoro and G. Petri, *Simplex2Vec embeddings for community detection in simplicial complexes*, preprint arXiv:1906.09068, 2019.
- [9] G. Boole, *The Mathematical Analysis of Logic: Being an Essay Towards a Calculus of Deductive Reasoning*, Cambridge University Press, 2009 (first published 1847).
- [10] G. Brockman, V. Cheung, L. Pettersson, J. Schneider, J. Schulman, J. Tang and W. Zaremba, *OpenAI Gym*, preprint arXiv:1606.01540, 2016.
- [11] F. Chazal and B. Michel, *An introduction to topological data analysis: fundamental and practical aspects for data scientists*, preprint arXiv:1710.04019, 2017.
- [12] R. Child, S. Gray, A. Radford and I. Sutskever, *Generating long sequences with Sparse Transformers*, preprint arXiv:1904.10509, 2019.
- [13] K. Cho, A. Courville and Y. Bengio, *Describing multimedia content using attention-based encoder-decoder networks*, in IEEE Transactions on Multimedia 17(11), 2015.
- [14] J. Clift and D. Murfet, *Cofree coalgebras and differential linear logic*, preprint arXiv:1701.01285v2, 2019.
- [15] J. Clift, D. Doryn, D. Murfet and J. Wallbridge, <https://github.com/dmurfet/2simplicialtransformer/>.

- [16] A. O. Constantinescu, J. X. O'Reilly and T. E. J. Behrens, *Organising conceptual knowledge in humans with a gridlike code*, Science 352, Issue 6292, pp. 1464–1468, 2016.
- [17] M. Dehghani, S. Gouws, O. Vinyals, J. Uszkoreit and L. Kaiser, *Universal transformers*, in Proceedings of the International Conference on Learning Representations (ICLR), 2019.
- [18] H. Dong, J. Mao, T. Lin, C. Wang, L. Li and D. Zhou, *Neural logic machines*, in Proceedings of the International Conference on Learning Representations (ICLR), 2019.
- [19] R. A. Epstein, E. Z. Patai, J. B. Julian and H. J. Spiers, *The cognitive map in humans: spatial navigation and beyond*, Nature Neuroscience, 2017.
- [20] L. Espeholt, H. Soyer, R. Munos, K. Simonyan, V. Mnih, T. Ward, Y. Doron, V. Firoiu, T. Harley, I. Dunning, S. Legg and K. Kavukcuoglu, *IMPALA: scalable distributed deep-RL with importance weighted actor-learner architectures*, preprint arXiv:1802.01561, 2018.
- [21] G. Frege, *On sense and denotation (Über Sinn und Bedeutung)*, Zeitschrift für Philosophie und philosophische Kritik, vol. 100 pp. 25–50, 1892.
- [22] C. L. Giles, G. Z. Sun, H. H. Chen, Y. C. Lee and D. Chen, *Higher order recurrent networks and grammatical inference*, in Advances in Neural Information Processing Systems (NeurIPS), 1989.
- [23] C. L. Giles, D. Chen, C. B. Miller, H. H. Chen, G. Z. Sun and Y. C. Lee, *Second-order recurrent neural networks for grammatical inference*, in IJCNN-91-Seattle International Joint Conference on Neural Networks Vol. 2, pp. 273–281 1991.
- [24] J. Gilmer, S. S. Schoenholz, P. F. Riley, O. Vinyals and G. E. Dahl, *Neural message passing for quantum chemistry*, in Proceedings of the International Conference on Machine Learning (ICML), 2017.
- [25] J. -Y. Girard, *Linear logic*, Theoretical Computer Science 50 (1), pp. 1–102, 1987.
- [26] I. Goodfellow, Y. Bengio and A. Courville, *Deep learning*, MIT Press, 2016.
- [27] M. W. Goudreau, C. L. Giles, S. T. Chakradhar and D. Chen, *First-order versus second-order single-layer recurrent neural networks*, IEEE Transactions on Neural Networks, 5(3), pp. 511–513, 1994.
- [28] A. Graves, G. Wayne and I. Danihelka, *Neural Turing machines*, preprint arXiv:1410.5401, 2014.

- [29] A. Graves, G. Wayne, M. Reynolds, T. Harlye, I. Danihelka, A. Grabska-Barwińska, S. G. Colmenarejo, E. Grefenstette, T. Ramalho, J. Agapiou, A. P. Badia, K. M. Hermann, Y. Zwols, G. Ostrovski, A. Cain, H. King, C. Summerfield, P. Blunsom, K. Kavukcuoglu and D. Hassabis, *Hybrid computing using a neural network with dynamic external memory*, Nature 538, pp. 471–476, 2016.
- [30] A. Guez, M. Mirza, K. Gregor, R. Kabra, S. Racanieère, T. Weber, D. Raposo, A. Santoro, L. Orseau, T. Eccles, G. Wayne, D. Silver and T. Lillicrap, *An investigation of model-free planning*, in Proceedings of the International Conference on Machine Learning (ICML), 2019.
- [31] P. Henderson, R. Islam, P. Bachman, J. Pineau, D. Precup and D. Meger, *Deep reinforcement learning that matters*, preprint arXiv:1709.06560, 2017.
- [32] D. Hestenes, *New foundations for classical mechanics*, 2nd edition, Kluwer Academic publishers 2002.
- [33] J. Hewitt and C. D. Manning, *A structural probe for finding syntax in word representations*, in Proceedings of the 2019 Conference of the North American Chapter of the Association for Computational Linguistics: Human Language Technologies, Volume 1 (Long and Short Papers), pp. 4129–4138, 2019.
- [34] J. J. Hopfield, *Neural networks and physical systems with emergent collective computational abilities*, Proceedings of the National Academy of Sciences of the USA, vol. 79 no. 8 pp. 2554–2558, 1982.
- [35] M. Hyland, *Game semantics*, Semantics and logics of computation 14, 1997.
- [36] O. Irsoy and C. Cardie, *Modeling compositionality with multiplicative recurrent neural networks*, in Proceedings of the International Conference on Learning Representations (ICLR), 2014.
- [37] M. Jaderberg, V. Dalibard, S. Osindero, W. M. Czarnecki, J. Donahue, A. Razavi, O. Vinyals, T. Green, I. Dunning, K. Simonyan and C. Fernando, *Population based training of neural networks*, preprint arXiv:1711.09846, 2017.
- [38] P. W. Koh and P. Liang, *Understanding Black-box predictions via influence functions*, in Proceedings of the International Conference on Machine Learning (ICML), 2017.
- [39] R. Lambiotte, M. Rosvall and I. Scholtes, *From networks to optimal higher-order models of complex systems*, Nature physics, 15 pp. 313–320, 2019.
- [40] E. Liang, R. Liaw, R. Nishihara, R. Moritz, R. Fox, K. Goldberg, J. E. Gonzalez, M. I. Jordan and I. Stoica, *RLlib: Abstractions for distributed reinforcement learning*, in Proceedings of the International Conference on Machine Learning (ICML), 2018.

- [41] Y. Liu, R. J. Dolan, Z. Kurth-Nelson and T. E. J. Behrens, *Human replay spontaneously reorganizes experience*, *Cell*, 178 pp. 1–13, 2019.
- [42] A. Macdonald, *Sobczyks simplicial calculus does not have a proper foundation*, preprint arXiv:1710.08274, 2017.
- [43] D. Mackay, *Information theory, inference and learning algorithms*, Cambridge University Press, 2003.
- [44] N. J. Mackintosh, *Animal learning*, Encyclopaedia Britannica, <https://www.britannica.com/science/animal-learning/Insight-and-reasoning>, access date July 15, 2019.
- [45] C. Martens, *Programming interactive worlds with linear logic*, Doctoral dissertation, Carnegie Mellon University, 2015.
- [46] K. Mavreshko (kpot), *keras-transformer*, <https://github.com/kpot/keras-transformer>.
- [47] P-A. Mellès, *Categorical semantics of linear logic*, in : Interactive models of computation and program behaviour, Panoramas et Synthèses 27, Société Mathématique de France, 2009.
- [48] A. Nguyen, J. Yosinski and J. Clune, *Multifaceted feature visualization: uncovering the different types of features learned by each neuron in deep neural networks*, in International Conference on Machine Learning (ICML), 2016.
- [49] C. Olah and S. Carter, *Attention and Augmented Recurrent Neural Networks*, Distill, <http://distill.pub/2016/augmented-rnns>, 2016.
- [50] J. B. Pollack, *The induction of dynamical recognizers*, *Machine Learning*, 7(2-3) pp. 227–252, 1991.
- [51] M. Ranzato, A. Krizhevsky and G. E. Hinton. *Factored 3-Way Restricted Boltzmann machines for modeling natural images*, AISTATS, 2010.
- [52] A. Santoro, D. Raposo, D. G. Barrett, M. Malinowski, R. Pascanu, P. Battaglia and T. Lillicrap, *A simple neural network module for relational reasoning*, in Advances in Neural Information Processing Systems (NeurIPS), 2017.
- [53] A. Santoro, R. Faulkner, D. Raposo, J. Rae, M. Chrzanowski, T. Weber, D. Wierstra, O. Vinyals, R. Pascanu and T. Lillicrap, *Relational recurrent neural networks*, in Advances in Neural Information Processing Systems (NeurIPS), 2018.
- [54] D. Raposo, *Personal communication*, May 13, 2019.

- [55] L. Serafini and A. Garcez, *Logic tensor networks: Deep learning and logical reasoning from data and knowledge*, in Proceedings of the International Workshop on Neural-Symbolic Learning and Reasoning (NeSy@HLAI), 2016.
- [56] A. Shrikumar, P. Greenside and A. Kundaje, *Learning important features through propagating activation differences*, in Proceedings of the International Conference on Machine Learning (ICML), 2017.
- [57] K. Simonyan, A. Vedaldi and A. Zisserman, *Deep inside convolutional networks: visualising image classification models and saliency maps*, in Proceedings of the International Conference on Learning Representations (ICLR), 2013.
- [58] R. Smith, *Aristotles Logic*, The Stanford Encyclopedia of Philosophy (Summer 2019 Edition), Edward N. Zalta (ed.), <https://plato.stanford.edu/archives/sum2019/entries/aristotle-logic/>, 2019.
- [59] G. E. Sobczyk *Simplicial calculus with geometric algebra*, in: Micali A., Boudet R., Helmstetter J. (eds) Clifford Algebras and their Applications in Mathematical Physics. Fundamental Theories of Physics, vol 47. Springer, Dordrecht, 1992.
- [60] R. Socher, D. Chen, C. D. Manning, and A. Ng, *Reasoning with neural tensor networks for knowledge base completion*, in Advances in Neural Information Processing Systems (NeurIPS), 2013.
- [61] P. V. Spade and J. J. Hintikka, *History of logic*, Encyclopaedia Britannica, <https://www.britannica.com/topic/history-of-logic/Aristotle>, access date July 15, 2019.
- [62] I. Sutskever, J. Martens and G. E. Hinton, *Generating text with recurrent neural networks*, in Proceedings of the International Conference on Machine Learning (ICML), 2011.
- [63] R. S. Sutton and A. G. Barto, *Reinforcement learning: an introduction*, 2nd edition, MIT Press, 2018.
- [64] C. Szegedy, V. Vanhoucke, S. Ioffe, J. Shlens and Z. Wojna, *Rethinking the Inception Architecture for Computer Vision*, Conference on Computer Vision and Pattern Recognition (CVPR), 2016.
- [65] T. Tieleman and G. Hinton, *Lecture 6.5 - RmsProp: Divide the gradient by a running average of its recent magnitude*, COURSERA: Neural Networks for Machine Learning, 2012.
- [66] A. Vaswani, N. Shazeer, N. Parmar, J. Uszkoreit, L. Jones, A. N. Gomez, L. Kaiser and I. Polosukhin, *Attention is all you need*, in Advances in Neural Information Processing Systems (NeurIPS), 2017.



- [67] O. Vinyals, I. Babuschkin, J. Chung, M. Mathieu, M. Jaderberg, W. Czarnecki, A. Dudzik, A. Huang, P. Georgiev, R. Powell, T. Ewalds, D. Horgan, M. Kroiss, I. Danihelka, J. Agapiou, J. Oh, V. Dalibard, D. Choi, L. Sifre, Y. Sulsky, S. Vezhnevets, J. Molloy, T. Cai, D. Budden, T. Paine, C. Gulcehre, Z. Wang, T. Pfaff, T. Pohlen, Y. Wu, D. Yogatama, J. Cohen, K. McKinney, O. Smith, T. Schaul, T. Lillicrap, C. Apps, K. Kavukcuoglu, D. Hassabis and D. Silver, *AlphaStar: Mastering the Real-Time Strategy Game StarCraft II*, <https://deepmind.com/blog/alphastar-mastering-real-time-strategy-game-starcraft-ii/>, 2019.
- [68] J. C. R. Whittington, T. H. Muller, S. Mark, C. Barry and T. E. J. Behrens, *Generalisation of structural knowledge in the hippocampal-entorhinal system*, in Advances in Neural Information Processing Systems (NeurIPS), 2018.
- [69] V. Zambaldi, D. Raposo, A. Santoro, V. Bapst, Y. Li, I. Babuschkin, K. Tuyls, D. Reichert, T. Lillicrap, E. Lockhart, M. Shanahan, V. Langston, R. Pascanu, M. Botvinick, O. Vinyals and P. Battaglia, *Deep reinforcement learning with relational inductive biases*, in Proceedings of the International Conference on Learning Representations (ICLR), 2019.

James Clift

*E-mail address:* jamesedwardclift@gmail.com

Dmitry Doryn

*E-mail address:* dmitry.doryn@gmail.com

Daniel Mufet

DEPARTMENT OF MATHEMATICS, UNIVERSITY OF MELBOURNE

*E-mail address:* d.murfet@unimelb.edu.au

James Wallbridge

*E-mail address:* james.wallbridge@gmail.com